https://doi.org/10.5194/egusphere-2026-3152
Preprint. Discussion started: 29 June 2026

Rapid mass loss and climate-driven dynamics of the Juvfonne ice patch, Norway (2010–2025)

Liss M. Andreassen[1], Ketil Isaksen[2], Lukas J. Monrad-Krohn[1,3,4], Jogscha M. Abderhalden[5,6], Luc Girod[4], Jessica De Marco[1], Bernd Etzelmüller[6], Simon Oldani[1], Rune Strand Ødegård[7]

[1]Section for Glaciers, Ice and Snow, the Norwegian Water Resources and Energy Directorate (NVE), Oslo, Norway
[2]Climate and Environment Department, Norwegian Meteorological Institute, Oslo, Norway
[3]Leipzig Institute for Meteorology, University of Leipzig, Leipzig, Germany.
[4]University of Oslo, Department of Geosciences, Oslo, Norway
[5]Western Norway University of Applied Sciences, Department of Civil Engineering and Environmental Sciences, Sogndal, Norway
[6]University of Bergen, Department of Earth Sciences, Bergen, Norway
[7]Norwegian University of Science and Technology, Gjøvik, Norway

Correspondence to: Liss M. Andreassen (lma@nve.no)

Abstract. Juvfonne is a small ice patch (~0.1 km^2) in Jotunheimen, southern Norway, and contains the oldest ice dated in Norway so far. More than 600 artefacts have been detected along the margin. Since 2010 annual investigations of mass balance with point measurements of snow accumulation and ablation have been carried out together with surface elevation and ice patch extent measurements. The outline mapping conducted between 2010 and 2025 demonstrates that the extent of Juvfonne undergoes continuous changes along the entire margin, varying from year to year. The decrease in area from 2010 to 2024 is 46% from 0.149 km^2 to 0.081 km^2. Ice thickness measurements conducted in September 2025 reveal a current maximum thickness of less than 9 meters and an interpolated mean thickness of < 3 meters. Repeat surface elevation surveys from lidar and UAV surveys reveal that Juvfonne has lost 73% of its volume between 2011 and 2025 and thinned on average 4 m (0.30 m a^{-1}), the value is sensitive to the outlines used. We compare the mass changes of Juvfonne with neighbouring glaciers in the Galdhøpiggen massif for the period 2011-2020 using repeated lidar surveys revealing that Juvfonne has had a smaller surface thinning than neighbouring glaciers over this period. Interpretation of data from two nearby automatic weather stations show that deposition of windblown snow on Juvfonne causes more snow accumulation than in the surroundings. The snow accumulation is dependent on wind direction and speed. Major snowfall events are associated with storms or synoptic cold fronts with westerly winds and short-term storm events can contribute greatly to the total accumulation. Ablation is related to cumulative positive degree days, but also to winter balance. Results from a Summer Melt Potential Index for the period 2010-2025 reveal a significant intensification of compounding melt events driven by the synergy of temperature, wind, and atmospheric moisture. Juvfonne prevails due to drifting snow and is controlled by topography and can fill up after years with surface lowering. However, the reduction in area and volume over the period 2010-2025 reveals that Juvfonne is vulnerable to the current warming and its current ice may completely vanish with a few warm summers.

https://doi.org/10.5194/egusphere-2026-3152
Preprint. Discussion started: 29 June 2026

1 Introduction

Glaciers come in a wide range of forms and sizes from small ice bodies to large valley glaciers and ice caps. The smallest glaciers and ice patches are often found in sheltered places where topographic conditions are favourable for the conservation of snow and ice such as depressions or gullies that receive additional accumulation from snow drift or avalanches (Kuhn, 1995; Nesje et al., 2011; De Marco et al., 2022; Davesne et al., 2023). Such bodies can exist below the regional glacier equilibrium line altitude (Arie et al., 2025) and have a self-regulating mechanism allowing them to survive (Fujita et al., 2010). The term ice patch is used for smaller ice bodies that may have been past glaciers but no longer exhibit forms of an active glacier (e.g. Serrano et al., 2011; Ødegård et al., 2017). Ice patches are small ice accumulations forming a transition between small glaciers and snow fields. They normally have no or very limited movement and can persist over long time periods. They are often cold-based, and therefore able to preserve artefacts lost on the ice over long periods. Archaeological finds from ice patches are known from North America, Mongolia, the European Alps and Scandinavia with numerous signs from hunting and travelling (Pilø, 2026). Knowledge of ice patches can be important for understanding spectacular finds such as skis (Finstad et al., 2018), or the Ötzi man (e.g. Pilø et al., 2022).

Early climate projections indicated that Scandinavia's higher elevations are likely to undergo the greatest warming across mainland northern Europe during the 21st century (Benestad, 2005; Benestad et al., 2016). Recent projections indicate that by the end of the century, Norway's average temperature will rise most in winter (3.9 °C from 1991–2002 to 2071–2100), with summer increases largest in southern mountain areas (Dyrrdal et al., 2025). Norway’s glaciers and ice patches are projected to experience substantial losses regardless of the degree of future warming due to the committed mass loss (Zekollari and others, 2025). Many glaciers are threatened to completely disappear (Van Tricht et al., 2025) and Norway’s northernmost and southernmost glaciers are already about to vanish (Andreassen et al., 2025; Winsvold et al., 2026).

Juvfonne (61°40′N, 8°21′E), is a small ice patch in Jotunheimen, southern Norway that has existed since the Holocene Thermal Maximum. Ice at the bottom has been dated to 7600 cal years BP (Ødegård et al., 2017). However, in recent decades the ice patch has retreated and thinned (Ødegård et al., 2017; Kjøllmoen et al., 2025). Around 600 archaeological finds and artefacts and 50 stone-made hunting blinds have been found in front of the retreating mass, the first find was made in 2007 (Nesje et al., 2011).

This study aims to provide a detailed understanding of the physical and climatic processes affecting Juvfonne. The specific objectives are: I) To assess changes in the mass balance (2010–2025), focusing on changes in surface elevation, ice thickness, volume, and extent. II) To evaluate snow accumulation patterns, with emphasis on the role of wind-driven redistribution and significant snowfall events. III) To analyse climate drivers influencing ice patch dynamics, including the effects of temperature, precipitation, wind, and solar radiation on melting and accumulation, as well as long-term trends in temperature, precipitation,

https://doi.org/10.5194/egusphere-2026-3152
Preprint. Discussion started: 29 June 2026

and humidity. IV) To discuss Juvfonne's behaviour within regional trends by comparing elevation and area changes with neighbouring glaciers. V) To evaluate Juvfonne's resilience to climate change, assess its ability to regain mass during favourable years and discuss the implications of ongoing and future climate change on its survival. The study provides new insights into the impacts of climate change on small ice bodies.

2 Study site

Juvfonne (61°40′N, 8°21′E) is a small ice patch situated in the Jotunheimen mountain massif in central southern Norway (Fig. 1). It is located close by Galdhøpiggvegen road, the highest elevated road in Norway reaching up to ~1850 m a.s.l. at the Galdhøpiggen summer ski centre on the glacier Vesljuvbrean with the Juvvasshøe and Juvflye meteorological stations (Fig. 1a). Juvfonne is included in the two most recent inventories based on satellite data (Andreassen et al., 2012; 2022), but not in previous inventories of southern Norway (Østrem et al., 1969; Østrem et al, 1988). The ice patch has an area of 0.086 km2 and altitudinal range from 1852 to 1985 m a.s.l. (map of 2019). Juvfonne is estimated to have had a thickness of 45-60 m at its little ice age (LIA) maximum and had a maximum thickness of 17-19 m in 2009 (Ødegård et al., 2017). The glaciological observation programme of Juvfonne started in 2010 and consists of glaciological surface mass balance, front position measurements and annual surveys of the glacier extent (e.g. Kjøllmoen et al., 2025).

The site is situated well within the mountain permafrost zone (e.g. Isaksen et al., 2022), where ice temperatures at 10 m depth and permafrost temperatures (outside the ice patch) typically range between -2 and -4 °C (Ødegård et al., 2017; Etzelmüller et al., 2023). This underlying permafrost provides a cold thermal regime that limits basal melting, playing a critical role in preserving the ice patch and its ancient internal structures for millennia (cf. Haeberli et al., 2004). Two tunnels have been excavated by hand with specially designed ice axes in the Juvfonne ice patch. The first one a 30 m tunnel in 2010 which melted out due to the retreat of the ice patch and then a second one in 2012 was excavated into the central and deepest parts of the ice patch (Ødegaard et al., 2017). Since 2016 geotextiles have covered the tunnel and caused an anthropogenic influence on the tunnel delaying the melt in this part (Fig. S1). Since 2024 snow has been redistributed over the tunnel to protect it. Organic material sampled in the ice tunnel has revealed ages from modern at the surface to ca. 7600 cal years BP at the bottom (Ødegård et al., 2017).

Juvvasshøe (1894 m a.s.l.) is a rounded mountain top about 800 m east of Juvfonne (Fig. 1). The Juvvasshøe climate monitoring site consists of two permafrost boreholes and an automatic weather station (AWS) measuring since September 1999 (Sollid et al., 2000; Fig. 1a, Fig. S2). The site became an official station in the national network of the Norwegian Meteorological Institute (MET Norway) in June 2009 (Isaksen et al., 2011; 2022). The site is part of the Juvlye permafrost observatory, which contains additional 6 boreholes within and outside of the altitudinal permafrost limit (Farbrot et al., 2011; Hipp et al., 2012; Etzelmüller et al., 2023).

https://doi.org/10.5194/egusphere-2026-3152
Preprint. Discussion started: 29 June 2026

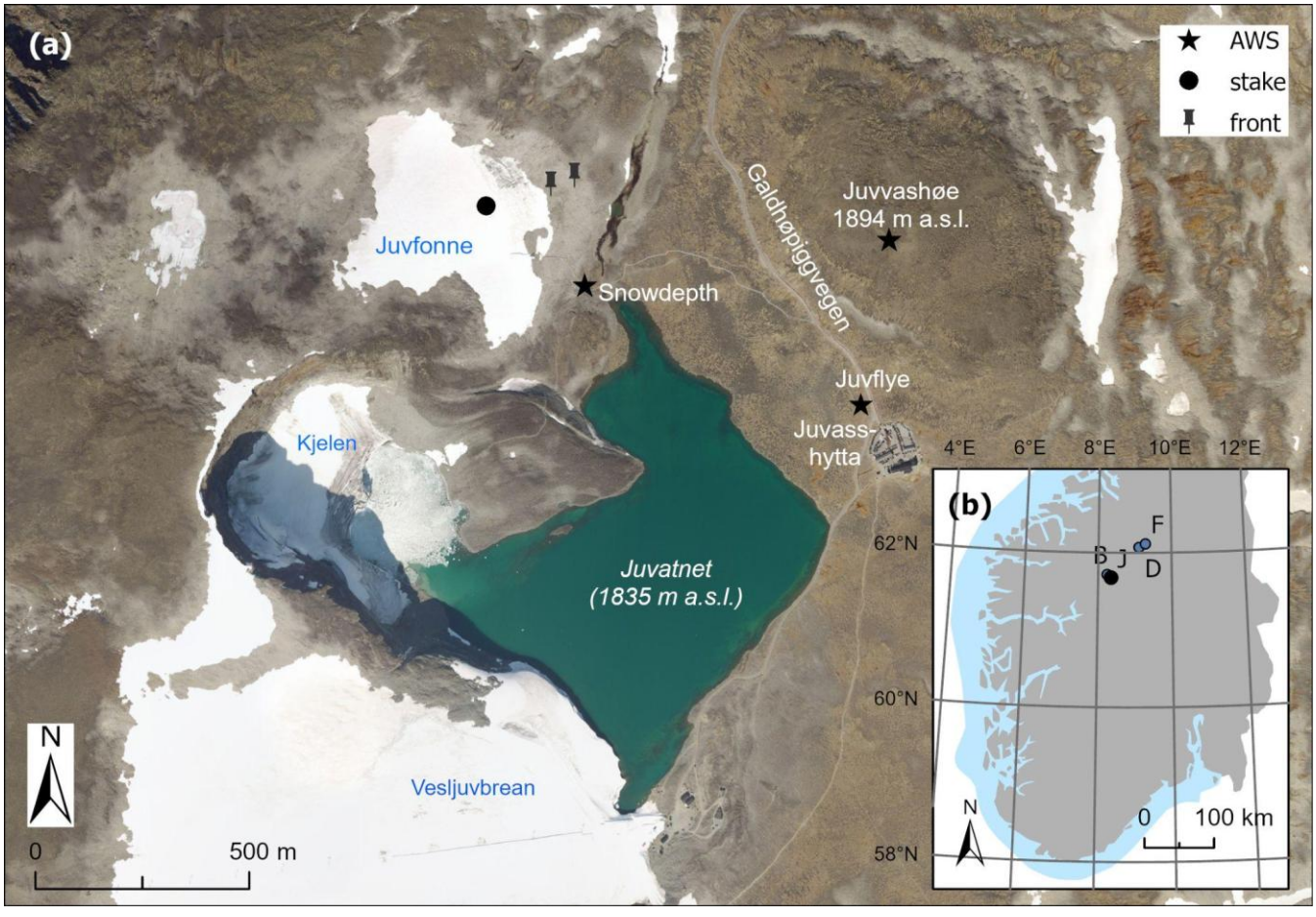

Figure 1: Location map of Juvfonne. (a) Juvfonne and surroundings including position of stake 2 and the automatic weather stations (AWS) on Juvvasshøe, Juvflye and the snow depth sensor and part of glacier Vesljuvbrean with its summer ski centre. Background orthophoto of 22 August 2017 from Norgeibilder.no. (b) Location of Juvfonne/Juvvasshøe (J) in southern Norway with additional weather stations B-Bøverdal, D-Dombås - Nordigard, F-Fokstugu. Coordinate system geographical on (b).

https://doi.org/10.5194/egusphere-2026-3152
Preprint. Discussion started: 29 June 2026

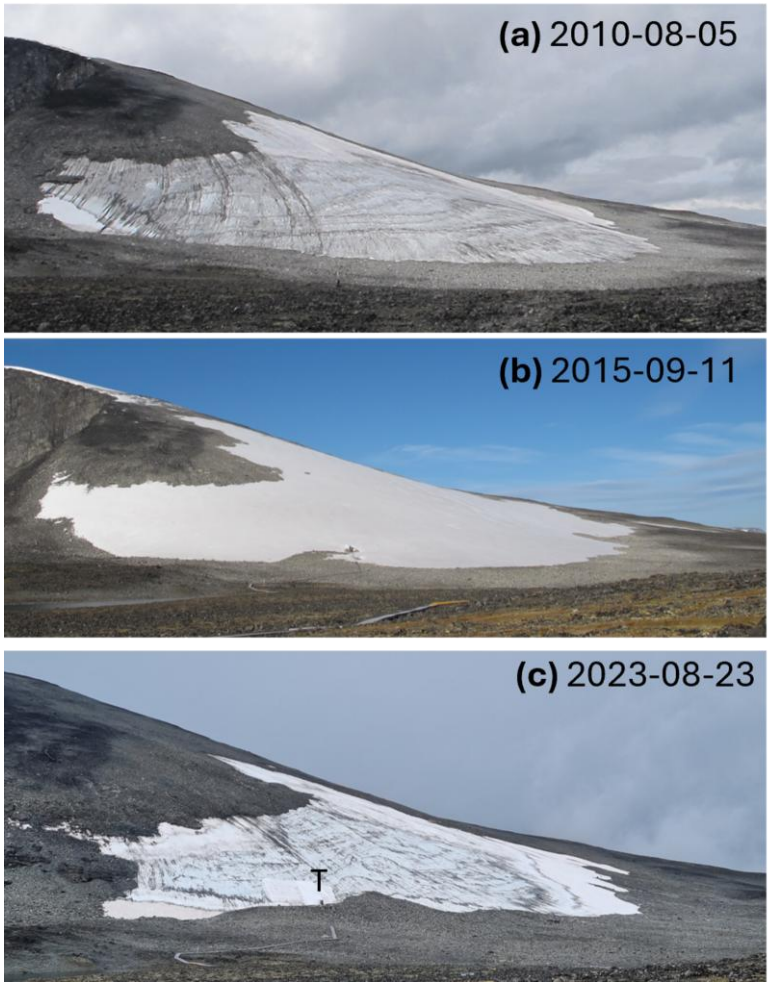

Figure 2: The Juvfonne ice patch has varied snow conditions through the years. (a) Nearly all snow had melted early August in the first observation year. (b) No ice exposed through the summer season in 2015. (c) Most of the snow vanished in late August 2023. T denotes the position of the tunnel that in 2023 is covered in geotextile (Fig. S1). Photos: Liss M. Andreassen.

3 Data and methods

3.1 Mass balance data

The mass balance programme of Juvfonne was initiated in spring 2010 and comprises winter balance measurements in 25-71 points, in addition to seasonal and annual balances derived from a single stake position (Fig. 1a). During the first year, up to 4 stake positions were monitored and a glacier-wide mass balance was calculated, but since 2011 observations have been limited to stake 2 at ~1880 m a.s.l. Winter accumulation and balance measurements are usually conducted in April or May, except in 2012 when measurements were performed on 11 June. Snow depth is measured by probing to the previous summer surface. In the initial years, measurements were collected along profiles, whereas since 2020 a fixed grid of 25 positions has been

https://doi.org/10.5194/egusphere-2026-3152
Preprint. Discussion started: 29 June 2026

measured (Fig. S3). Snow density is determined from a pit near the stake (Fig. 1a), with additional measurements of remaining snow density in September 2015. Stake readings are carried out in spring, summer and autumn, with measurements from September or October used to derive summer and annual balances. Spatial patterns in snow accumulation pattern were analysed using the "Getis-Ord Gi*" method (Getis and Ord, 1992; Ord and Getis 1995). Snow depth values were normalised as deviation from annual mean, and the analysis was conducted using a fixed bandwidth of 300 m. False discovery rate corrections were not applied.

3.2 Ice patch extent

The extent of Juvfonne has been regularly mapped since 2010 using differential GNSS or handheld GPS conducted on foot (Ødegård et al., 2017; Kjøllmoen et al., 2025). Measurements represent the outermost continuous boundary of snow or ice. Additional outlines were derived by digitising orthophotos from drone surveys (2021, 2022, 2023, 2024, 2025) and aerial imagery (2011, 2019) (Table S1), with multiple outlines for some years. Surveys were typically carried out in August or September. Surveys in 2012, 2018 and 2020 were incomplete due to snow conditions and covered only along the lower margin (Table S1). Since 2010, front position has also been monitored using distance measurements along sight lines from fixed points outside the ice patch, one established in 2010, and a second in 2021 closer to the terminus following retreat (Fig. 1a).

3.3 Surface elevations surveys

Surface elevations of the ice patch and surrounding terrain were mapped by lidar in 2011, 2019, and 2020 (Table S2). In 2011 and 2019, vertical aerial photographs were also acquired and used to generate orthophotos with a spatial resolution of 0.25 m. The lidar point clouds were used to derive digital terrain models (DTMs) with a spatial resolution of 1 m. Quality control and accuracy assessment showed that the vertical accuracy of the surface elevations was generally better than ±0.1 m. Additional surface-elevation data were obtained from UAV surveys. Here, we use surveys from 2016, 2023, and 2025 to assess the temporal evolution of surface-elevation change at Juvfonne. The 2016 survey was carried out on 13 September using an eBee UAV and yielded 208 photographs covering 0.856 km2 (Fig. 4c). Five ground-control points were established and surveyed using GNSS. Point-cloud processing and DTM generation were performed in Pix4D and CloudCompare, as described by Andreassen and De Marco (2018). The 2023 survey was carried out on 31 August without ground-control points, and point-cloud processing and DTM generation were performed in Pix4D. The 2025 survey was conducted using a DJI Matrice 4E connected to Kartverket's CORS network for RTK positioning. Real-time terrain following was used with a target altitude of 70 m above ground level, yielding 595 images with an approximate ground sampling distance (GSD) of 2 cm and a coverage of 0.389 km^2. Owing to dark and overcast conditions during the flight, the final output resolution was set to 5 cm GSD for the orthoimage and 10 cm GSD for the DSM. Processing was performed in Agisoft Metashape using only direct georeferencing from the image metadata. All UAV surveys were co-registered to the 2019 lidar survey. The accuracy of the 2023 and 2025

https://doi.org/10.5194/egusphere-2026-3152
Preprint. Discussion started: 29 June 2026

surveys is estimated to be within 0.1 m, with the 2016 survey suffering from some doming and have lower accuracy. In addition, the 2011 and 2020 lidar surveys that covered a larger section, the Galdhøpiggen massif, were used to calculate elevation change over this larger sample of glaciers. Glacier outlines for 2011 were manually digitised from orthophotos. For 2020, no orthophotos were available. We therefore used digital glacier outlines from the national inventory based on Sentinel-2 imagery from August 2019 (Andreassen et al., 2022), except for Kjelen and Juvfonne that were digitised orthophotos acquired on 26 August 2019 (See Table 1 for details). For all DTM pairs, DTM differencing was conducted in ArcGIS Pro by subtracting the newest DTM from the oldest in each pair. Mean elevation change was calculated over the combined glacier outlines from the first and second survey in the pair.

3.4 Ice thickness

Ice-patch thickness was surveyed in two independent campaigns in September 2025. On 3 September, measurements were acquired using a Zond Aero LF with a 300 MHz unshielded dipole antenna suspended beneath a DJI M300 RTK drone connected to Kartverket's CORS network for RTK positioning. A radar altimeter mounted on the gimbal was used to maintain a flight height of 2 m above ground level. Survey lines were spaced 25 m apart, and the target flight speed was 1.5 m s^{-1}.

On 24 September, measurements were acquired using a Malå ProEx unshielded rough-terrain antenna with a 100 MHz centre frequency. Ground-penetrating radar (GPR) data were collected by towing the antenna while walking at approximately constant speed. Global Navigation Satellite System (GNSS) positions along the survey lines were recorded with a G-Star IV BU-353S4 receiver, with a horizontal accuracy of < 2.5 m and a sampling interval of 0.2 s. This yielded a mean trace spacing of 0.15 ± 0.03 m. Each trace was stacked eight times to improve signal-to-noise ratio. Data were processed and analysed in ImpDAR, an open-source toolbox for impulse-radar processing and interpretation (Lilien et al., 2020). Processing included time-zero correction, vertical band-pass filtering, normal moveout correction for antenna separation, and range-gain application. Because surface slopes were gentle, we did not apply migration. Bedrock reflection travel times were converted to depth assuming a constant radio-wave velocity of 168 m μs^{-1}, a commonly used value for glacier ice (e.g. Navarro and Eisen, 2009; Gillespie et al., 2024). Previous measurements were also made in September 2009 (see Ødegård et al., 2017, for details).

To assess uncertainty, we compared overlapping measurements and obtained a mean crossover error of 0.72 ± 0.41 m, with a maximum discrepancy of 2.13 m at crossing points. We also estimated vertical and horizontal measurement errors following Lapazaran et al. (2016), yielding mean errors of 0.6 ± 0.41 m for ground-based measurements and 0.07 ± 0.03 m for drone-borne measurements. The 21 d interval between the two surveys in September 2025 likely introduced additional uncertainty because both melt and snowfall may have occurred between campaigns. At the time of the ablation measurements on 24 September 2025, a thin, uneven snow layer of 1–22 cm covered the ice patch at the stake location.

https://doi.org/10.5194/egusphere-2026-3152
Preprint. Discussion started: 29 June 2026

3.5 Meteorological data

We used meteorological data from the MET Norway observation network, including three stations in the vicinity of Juvfonne (Fig. S2) and three additional stations located farther away (Fig. 1a,b; Table S3). Model data were also included. Juvvasshøe (1894 m a.s.l.) is a full meteorological station situated within the elevation range of Juvfonne and measures air temperature, humidity, air pressure, wind speed and direction, and incoming and outgoing shortwave and longwave radiation (Isaksen et al., 2022). The station was originally installed in 1999 as a simple 3 m high AWS (Isaksen et al., 2003) and was upgraded in 2009 to a full-scale AWS with standard 10 m wind measurements. Owing to its location at the summit of Juvvasshøe, the station is exposed in all directions, and orographic wind effects are assumed to be minor. For periods with missing observations in 2023, air temperature and wind speed data at Juvvasshøe were gap-filled using linear regression based on data from the nearby automatic weather station on the Juvflye plateau (1844 m a.s.l.), close to the Juvasshytta cabin (Fig. 1a). Cumulative positive degree days (CPDD) were calculated from daily mean temperatures at Juvvasshøe for each year, beginning on 1 January. We also calculated the cumulative Summer Melt Potential Index, defined as a function of hourly sensible and latent heat exchange, using observations of air temperature, relative humidity, and wind speed in a simplified bulk aerodynamic approach (e.g., Hock, 2005; Ohmura, 2001). A sonic snow depth sensor (SR50A, Campbell Scientific, USA) was installed adjacent to Juvfonne, approximately 620 m southeast of stake 2 (Fig. 1a), in autumn 2011 (Ødegård et al., 2017). We used quality-controlled data from MET Norway, in which temperature measurements are applied to correct distance readings for the temperature-dependent speed of sound (Campbell Scientific Technical Communications, 2021). All values between 0 cm and the upper boundary just below the instrument height are checked, and a leap test is used to identify anomalously high values. Snow depths below 2 cm are set to 0 cm. In addition, MET Norway performs manual quality control to remove or interpolate flagged errors. Except for one extended gap from 11 January 2019 to 7 March 2020, the record consists of continuous hourly data. A further nine values were removed manually because they were unrealistically high, abrupt, and inconsistent with surrounding observations. To analyse longer-term variability, we used Fokstugu (973 m a.s.l.), Dombås–Nordigard (638 m a.s.l.), and Bøverdal (700 m a.s.l.), which provided climate normals and a basis for comparison with Juvvasshøe data (Table S3). Bøverdal is located 8 km northwest of Juvfonne, whereas Dombås–Nordigard and Fokstugu are situated 59 and 68 km to the northeast, respectively (Fig. 1b).

Complimentary data used for validation of derived data or parameters that are not measured are modelled data for one or a few representative grid points. The two used datasets are seNorge_2018 and NORA3. The seNorge_2018 version data set contains reanalysis data of minimum, maximum and daily mean temperature and precipitation from 1957 to present (Lussana et al., 2019). The data is calculated by interpolating observations to a 1km × 1km grid of Norway. As wind, temperature and precipitation are strongly dependent on elevation, the elevation of each grid point is accounted for in the interpolation. Snow data, such as snow depth or fresh snow water equivalent, are calculated from air temperature and precipitation data with the

https://doi.org/10.5194/egusphere-2026-3152
Preprint. Discussion started: 29 June 2026

seNorge snow model on the same grid and with a simplified data assimilation (Saloranta, 2016). NORA3 represents a high-resolution hindcast dataset that outperforms both the reanalysis ERA5 and the previous hydrostatic 10-km Norwegian Hindcast Archive (NORA10), particularly in areas of complex terrain (Haakenstad and Breivik, 2022).

3.6 Other data

A webcam overlooking the Galdhøpiggen summer ski centre on Vesljuvbrean and the adjacent mountainside (Fig. 1a; Fig. S4) was used as an independent reference for surface conditions near Juvfonne (gpss.no). Images were provided by the ski centre through NVE for January–November 2020. We compared the imagery with albedo at the Juvvasshøe weather station, defined as the ratio of incoming to outgoing shortwave radiation, to distinguish between bare ground and snow-covered conditions around the glacier. Based on this comparison, we used an albedo of 0.10 as an approximate threshold for bare ground and 0.15 as a threshold for snow cover exceeding 50% of the surface. The higher threshold was used because albedo is highly sensitive to small amounts of snow on bare rock.

4 Results

4.1 Mass balance data

Seasonal surface mass balance has been measured at stake 2 since 2010 (Fig. 3). Over 2010–2025 (16 years), the mean point winter balance was 1.37 ± 0.15 m w.e., and the mean point summer balance was −2.34 ± 0.15 m w.e. The cumulative mass balance at stake 2 over this period was −15.1 m w.e., corresponding to −0.94 m w.e. a^{-1}. Mass balance for the entire ice patch was not calculated for all years, but only for the first year of measurements (2009/2010), when more stakes were available. The smallest winter balance was measured in 2010 (0.71 m w.e.) and the largest in 2025 (2.10 m w.e.). Winter balance was generally lower during 2010–2016 (mean 1.10 m w.e.) than during 2017–2025 (mean 1.65 m w.e.). The most negative summer balance was recorded in 2010 (−3.99 m w.e.), and the smallest in 2015 (0.89 m w.e.). The largest annual deficits occurred in 2010 (−3.29 m w.e.) and 2014 (−2.30 m w.e.).

https://doi.org/10.5194/egusphere-2026-3152
Preprint. Discussion started: 29 June 2026

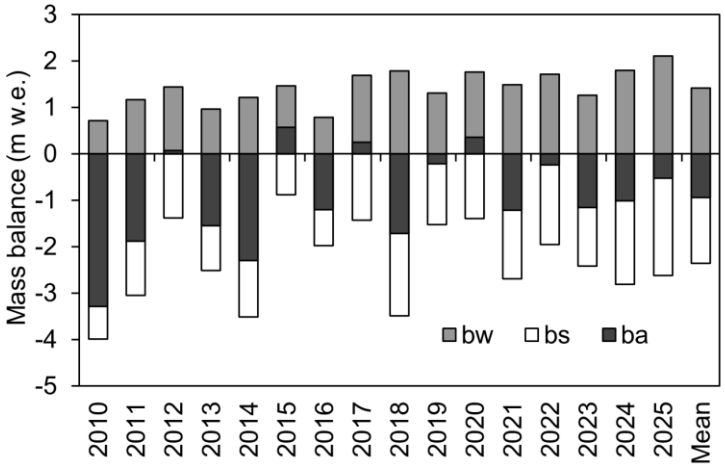

Figure 3: Point mass balance at stake 2 at Juvfonne 2010-2025 and the mean, given as winter balance (bw), summer balance (bs) and annual balance (ba).

4.2 Ice patch extent and front variation

Orthophotos and detailed annual glacier outline mapping document pronounced variability in the extent of Juvfonne over the period 2010-2025 (Fig. 4-5, Table S1). The mapped extent varies along the entire margin, with both expansion and shrinkage observed. In some years (e.g. 2016 and 2017; Fig. 4c-d), the upper parts expanded due to persistent snow along the perimeter, while the western parts increased between 2015 and 2018 (Fig. 5). In contrast, in 2019 the ice patch was entirely snow-free at the time of observation (4e). In subsequent years, the extent initially increased and then decreased. The largest extents were recorded in 2015 (0.186 km^2; Fig. 2b) and 2017 (0.183 km^2; Fig. 4d), when the ice patch was fully snow-covered (Table S1), whereas the smallest extents were recorded in 2019 (0.086 km^2; Fig. 4e) and 2024 (0.081 km^2; Fig. 4g). This corresponds to a reduction in area of 46% from 2010 to 2024. However, the relative area change is sensitive to the choice of reference year; using 2023 or 2025 yields reductions of 40% and 39%, respectively, reflecting the influence of transient snow cover along the margins. The estimates are also sensitive to survey timing, as early-season observations may not capture the annual minimum extent. For example, in 2011 a field survey on 2 August yielded an area of 0.150 km^2, whereas an orthophoto from 17 September indicated 0.127 km^2 (a 15% reduction). Conversely, fresh snowfall can obscure the margin and complicate delineation. Overall, Juvfonne has decreased in area from 2010 to 2025, with the most pronounced retreat occurring in the lower southwestern parts, but also affecting the upper parts, resulting in a modified overall geometry. Frontal variation measurements indicate a net retreat of 136 meters over the same period (9 m a^{-1}). Apparent advances in 2012, 2015 and 2020 are attributed to snow cover at the margin. Refreezing of meltwater under sub-freezing conditions can form a thin ice veneer along the edge. Juvfonne is presently too thin to sustain glacier flow and exhibits no significant dynamic movement.

https://doi.org/10.5194/egusphere-2026-3152
Preprint. Discussion started: 29 June 2026

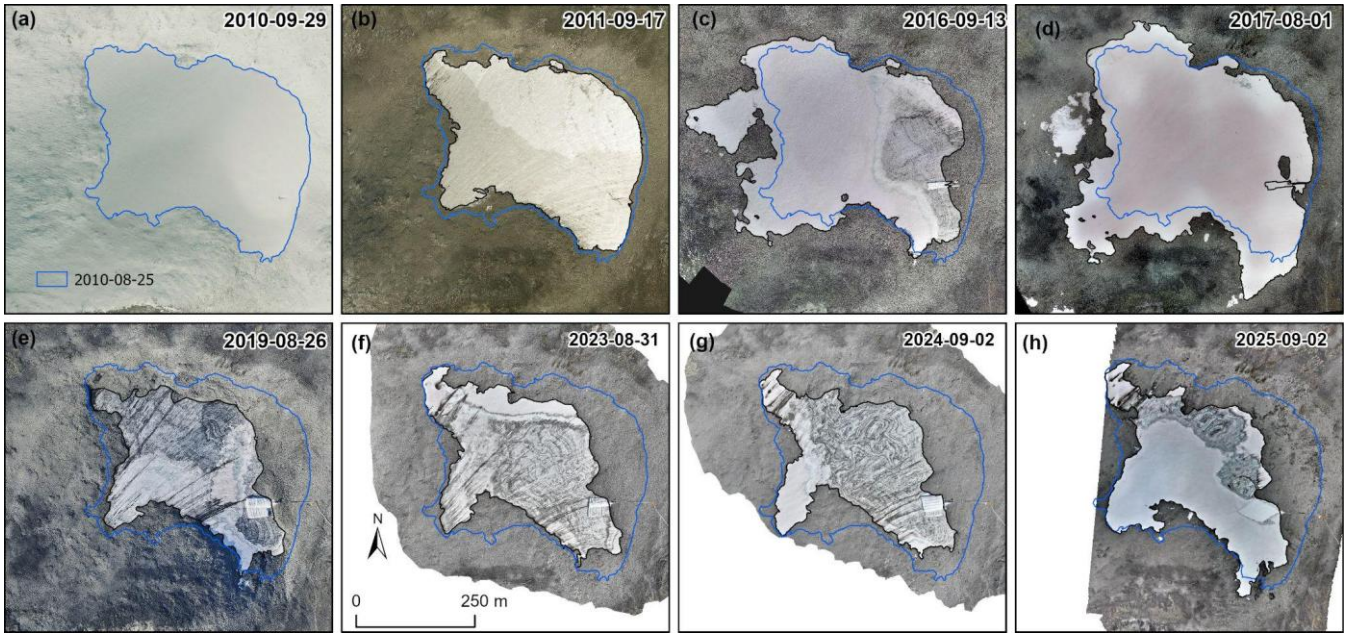

Figure 4: Orthophotos of Juvfonne from 2010 to 2025. Source (a) norgeibilder.no. (b) COWI. (c), (d), (f), (g) NVE UAV. (e) TerraTec (h) DroneLab@UiO UAV. The outline from the GNSS survey on 25 August 2010 is shown on all orthophotos. For years 2011-2025 the outline digitised from the orthophoto date is shown in black. See also Table S1 and S2.

https://doi.org/10.5194/egusphere-2026-3152
Preprint. Discussion started: 29 June 2026

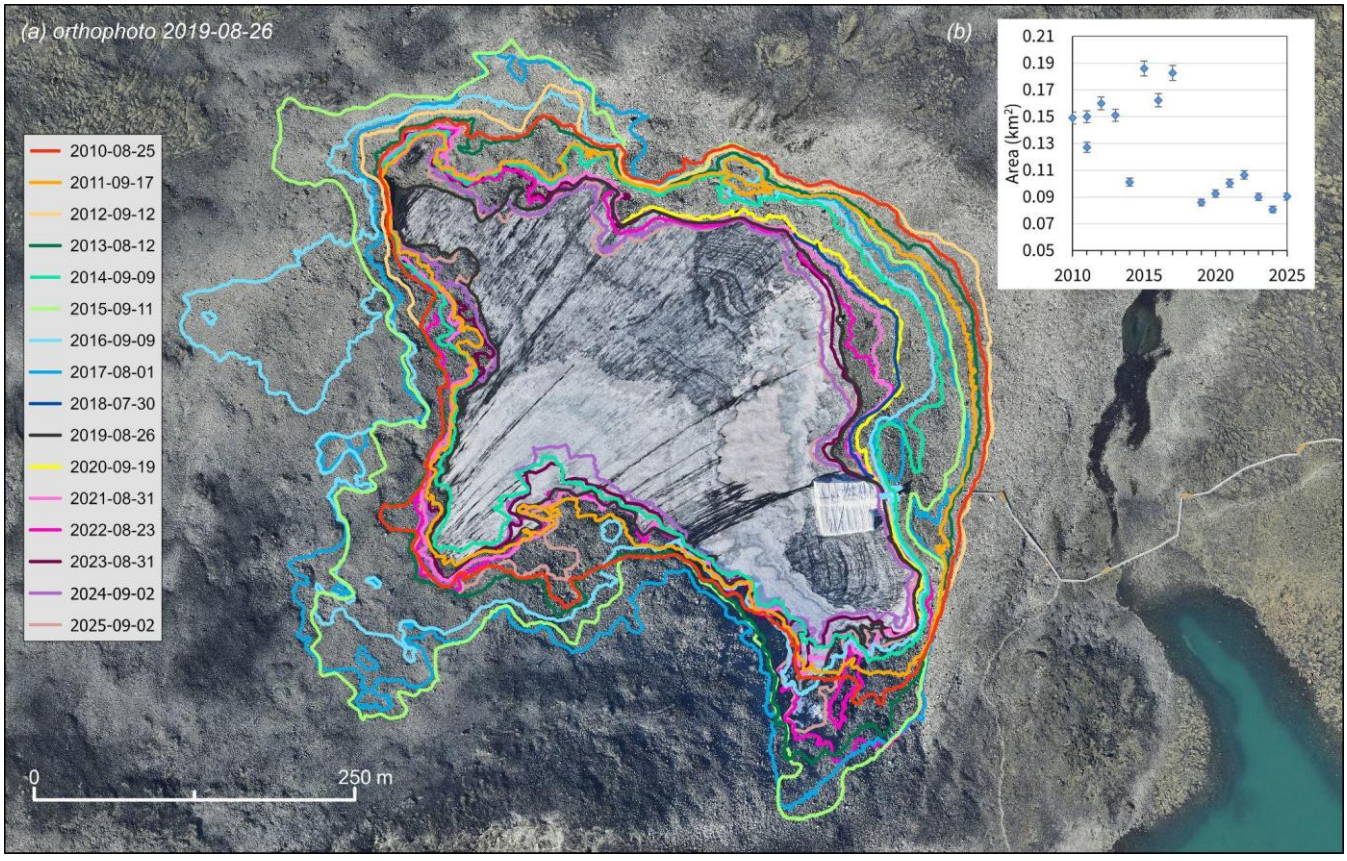

Figure 5: a) Variation of the ice extent of Juvfonne from 2010 to 2025. Background orthophoto of 26 August 2019. The walking path to the ice patch and the fabric covered ice tunnel is visible in the photo. The extent outlines are measured by orthophotos, differential GNSS and handheld GPS. Note that extents in 2012 and 2020 are partly based on extents from 2011 and 2019 (See Table S1). (b) Area of Juvfonne from outlines 2010-2025 shown in (a) with uncertainty bars.

4.3 Changes in surface elevation

DTM differencing of the lidar and UAV surveys reveals changes in the surface elevation over several subperiods (Fig. 6). During 2011–2016, Juvfonne thickened in the upper parts and thinned in the lower parts (Fig. 6a), likely due to residual snow cover in 2015 and 2016. In contrast, during 2016–2019, thinning and retreat affected nearly the entire ice patch (Fig. 6b). Over the full lidar period 2011–2019, most of Juvfonne experienced surface lowering, except for the highest parts, and the snowfields present in 2016 had disappeared by 2019 (Fig. 6c). The mean surface elevation change for Juvfonne was −3.1 m (−0.39 m a^{-1}), calculated over the combined extent of 2011 and 2019, with values ranging from 0.71 m to −10.2 m and a median of −2.5 m. At stake 2, the surface lowered by ~6 m, while at the tunnel roof it was ~4 m lower in 2019 than in 2011, indicating the effect of the geotextile installed in 2016. Between 2019 and 2023, thinning continued across most of the ice patch (Fig. 6d). Over the last period 2023-2025 the glacier shrunk in the lowermost parts but thickened in uppermost parts (Fig. 6e). During 2023–2025, thinning persisted in the lowermost parts, whereas the uppermost areas showed thickening (Fig. 6e). Over the full

https://doi.org/10.5194/egusphere-2026-3152
Preprint. Discussion started: 29 June 2026

period from 17 September 2011 to 2 September 2025, Juvfonne thinned overall, except for limited parts at the highest elevations (Fig. 6f). The mean elevation change was −3.80 m (−0.27 m a^{-1}) based on the combined 2011 and 2025 extent. Using the 2011–2023 extent instead yields a mean thinning of −4.15 m (−0.30 m a^{-1}), highlighting the sensitivity of results to the choice of spatial mask. At stake 2, the cumulative surface lowering is ~10 m, while at the upper part of the geotextile-covered tunnel roof the surface is ~7 m lower in 2025 than in 2011. The influence of the geotextile is clearly visible in the elevation difference maps (Fig. 6), particularly during 2023–2025, when snow redistribution over the tunnel produced apparent thickening (Fig. 6e). This artificial effect locally reduces the observed thinning relative to the surrounding areas.

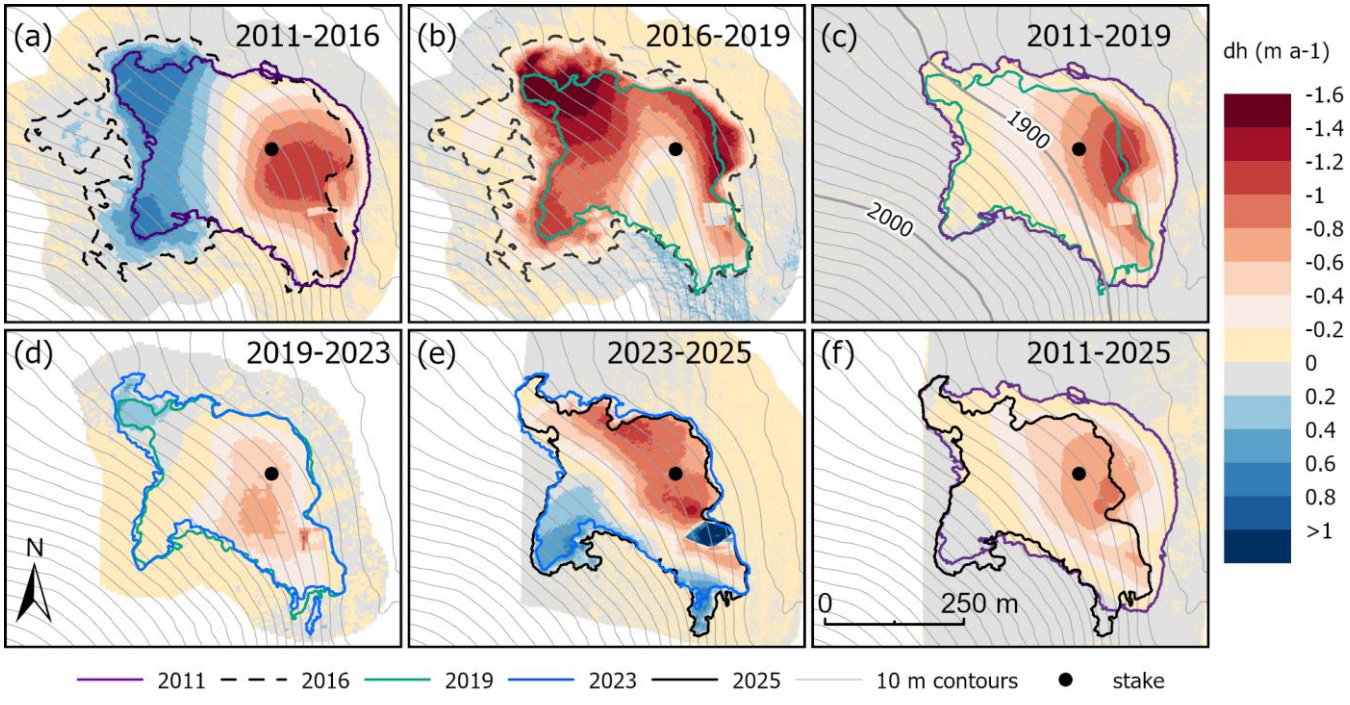

Figure 6: Elevation difference (m a^{-1}) for several periods of Juvfonne based on repeat laser scanning (2011, 2019) and UAV surveys (2016, 2023, 2025). Contours 10 m from 2011 are shown on (a)-(f) for reference, with 100 m contours labelled in (c). See Table S2 for details on surveys.

4.4 Ice thickness

Ice thickness measurements indicate a maximum thickness of 8.3 m located in the upper southwestern part of the current ice patch extent (Fig. 7), southwest of the present tunnel. The mean ice thickness of the measured points is 3.5 ± 0.6 m. Interpolation of the ice thickness measurements over the 2024-2025 minimum extent yields a mean thickness of 2.52 m, increasing to 2.88 m when restricted to areas within 50 m from measured points. At the stake location, the ice thickness is 3.3

https://doi.org/10.5194/egusphere-2026-3152
Preprint. Discussion started: 29 June 2026

m (Fig. 7a). The maximum ice thickness measured in 2009 was 17–19m (Ødegaard et al., 2017). Although the 2009 and 2025 measurements were not collected along identical profiles, the comparison clearly indicates substantial thinning.

Based on a current (2025) volume of 20 m^3 and an estimated volume of 73 m^3 in 2011, Juvfonne has lost approximately 73% of its volume in this period.

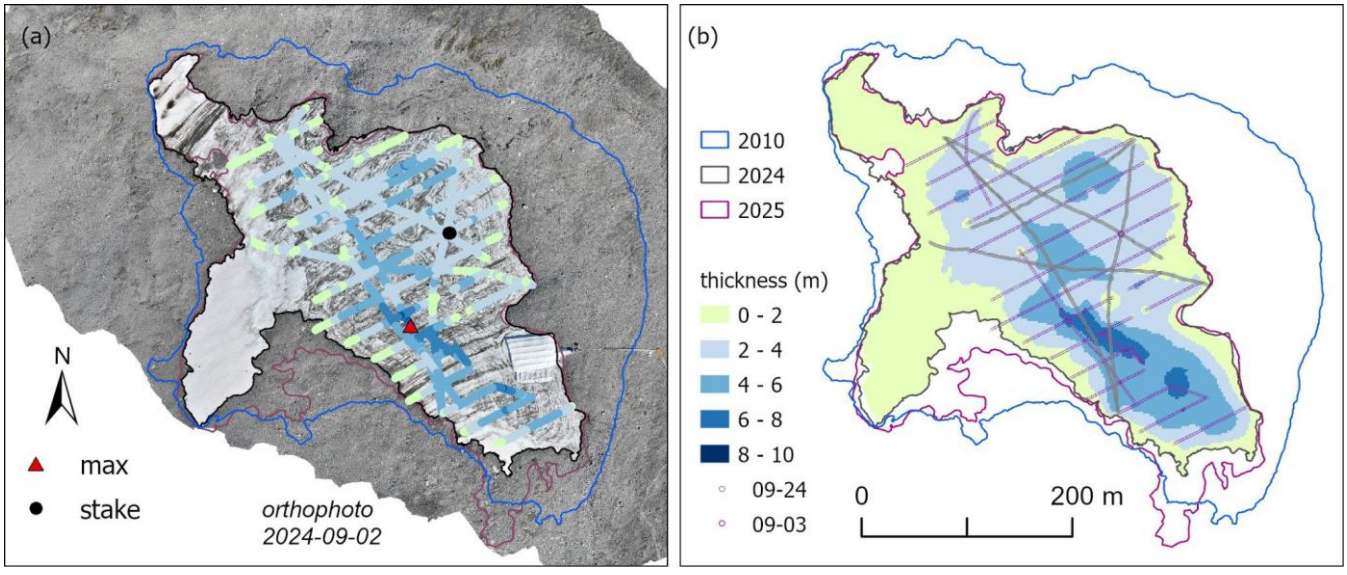

Figure 7: (a) Ice thickness (m) measured on 3 and 24 September 2025 with the maximum thickness (max) marked. (b) Interpolated ice thickness (m) within the minimum 2024 and 2025 extent and point data from 24-09 campaign (star pattern in grey) and 03-09 (regular lines in purple). Background orthophoto on (a) from 2 September 2024 with the tunnel roof covered in white geotextile. The outlines from 25 August 2010, 2 September 2024 and 2 September 2025 are shown on both (a) and (b).

4.5 Snow accumulation patterns

The annual snow depth surveys over 2010-2023 reveal differences in the annual snow accumulation (Fig. S3). The mean of all the 516 soundings is 2.81 m, and the mean snow thickness in each year varies between 1.49 m in 2019 and 5.12 m in 2020. The maximum snow depth was measured in 2020 with 5.78 m. The snow depths minimum and maximum are similar to the bw measured at stake 2. Over this 14-year period there is more accumulation of snow at lower altitude in the east and south-east, indicated by “hot spot” red markers in Fig. 8. This area typically accumulates drifting snow at westerly or north-westerly wind directions. This means that increased melting at low altitude is partly compensated with more accumulation. However, the late season snow measurements show great interannual variability in the pattern of accumulation. The geotextiles covering the tunnel since 2016 (Fig. S1) may also have affected the snow distribution, as this caused the tunnel to rise above the other parts due to less melting here, a pattern that has become more pronounced in recent years due to retreat and thinning of the ice patch (Fig. 6). We did not include the two last years of record, 2024 and 2025, where snow was redistributed to protect the ice tunnel.

https://doi.org/10.5194/egusphere-2026-3152
Preprint. Discussion started: 29 June 2026

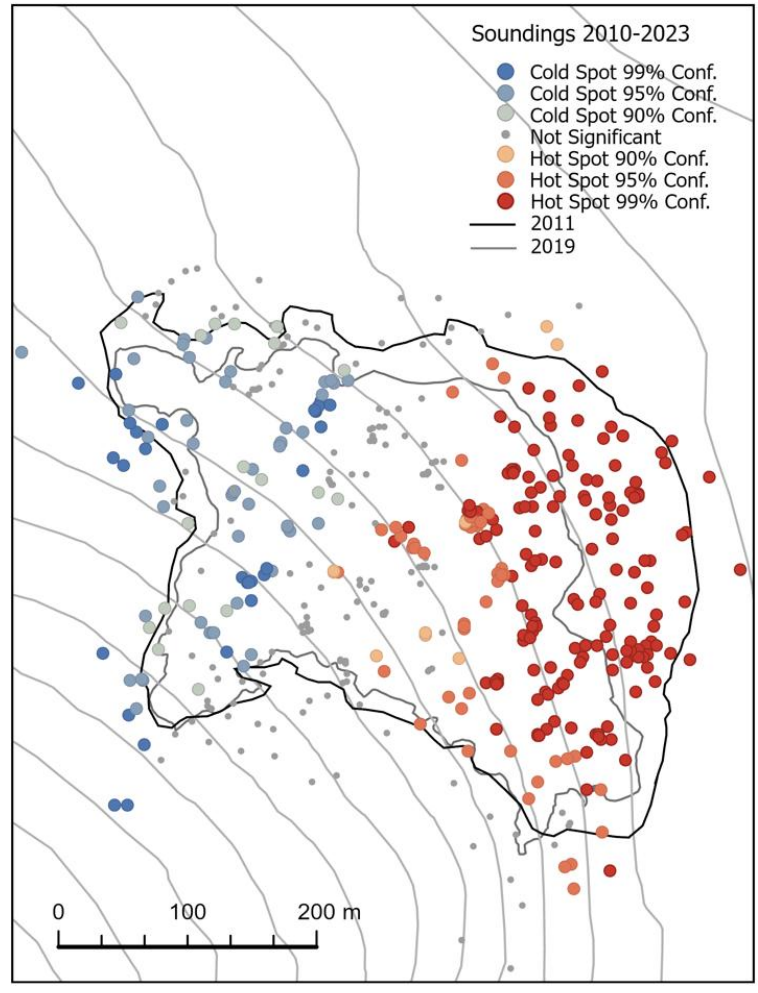

Figure 8: The 516 snow depth measurements from Juvfonne from the period 2010-2023 analysed by the "Getis-Ord Gi*" method. See Fig. 5a for annual extent fluctuations and Fig. S3 for annual snow depth measurements.

Whereas the snow accumulation at Juvfonne is measured once a year in spring, the nearby AWS records snow depth continuously at hourly intervals. Comparison between snow depth at mass balance stake 2 and measurements from the station located 600 m away, outside the ice patch (Fig. 1a), shows that snow accumulation on Juvfonne is typically three to four times greater than at the station, increasing to up to six times greater in 2018 and 2020 (Fig. S5).

The consistently higher accumulation at Juvfonne relative to the nearby sensor reflects strong spatial variability in snow distribution. This is primarily driven by wind transport of snow from the surrounding terrain and subsequent deposition on the ice patch.

https://doi.org/10.5194/egusphere-2026-3152
Preprint. Discussion started: 29 June 2026

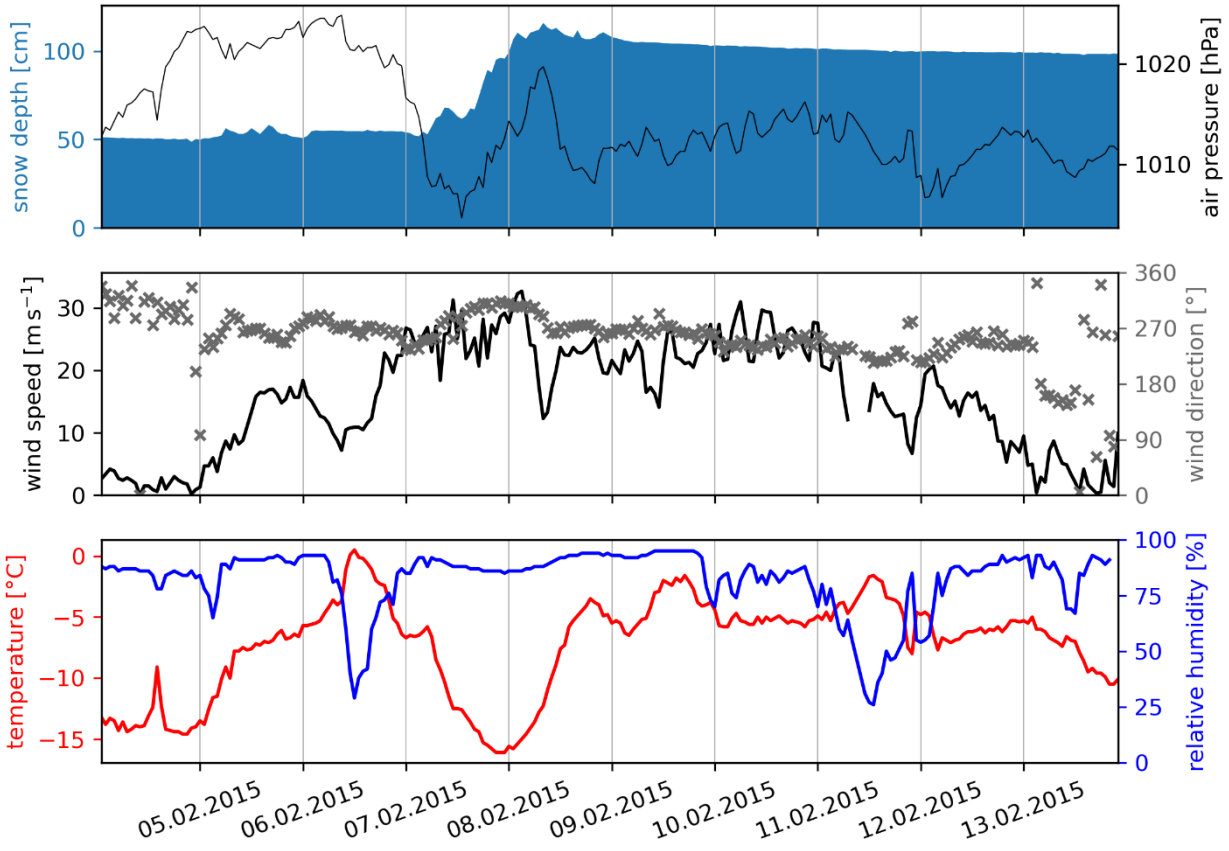

Figure 9: The time series shows meteorological data ((a) snow depth and air pressure, (b) wind speed and direction, (c) air temperature and relative humidity) of Juvvasshøe around before and after a cold front.

Analyses of the snow depth data revealed several events of strong increase of snow depth in a short time period of 1-3 days. As an example, in February 2015 half of the total annual snow fell within 24 hours (Fig. 9). The meteorological conditions around this period indicate the passing of a cold front shortly before the snowfall. Before 7 February the air mass at Juvfonne was warm and humid with a high sea level air pressure. The peak in air temperature and relative humidity on 6 February is probably caused by warming due to insolation. In the morning of 7 February the air pressure has dropped by around 10 hPa, the wind direction abruptly shifts to a more northerly direction and the air temperature begins to fall. These three criteria mark the passage of the cold front at the surface. There is a short period of one day with cold and humid conditions and heavy snowfall, before a warm front passes around noon on 8 February. At this point the wind direction changes back to west and the air temperature stays at around -5°C. The warm front also brings a small decrease in snow depth.

https://doi.org/10.5194/egusphere-2026-3152
Preprint. Discussion started: 29 June 2026

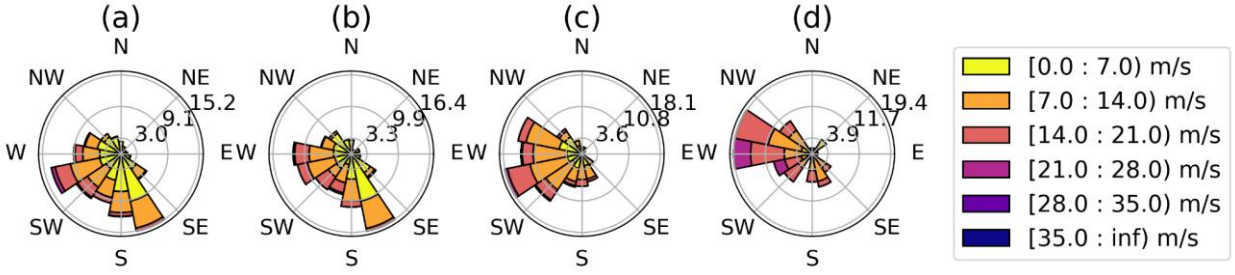

Figure 10: The windroses show the occurrence frequency (in %) of wind direction and speed for days with (a) no snowfall (3387 days), (b) less than 2 cm snowfall (574 days), (c) 2-10 cm snowfall (325 days) or (d) more than 10 cm of fresh snow (73 days). The data period is December 2011 to December 2022.

The high snowfall caused by a cold front is no isolated case. Between 2011 and 2022, we identified more than 20 similar, although mostly weaker, events (not shown). A combination of wind data from Juvvasshøe and the snow depth reveals that the main wind direction at Juvvasshøe is westerly and southerly to south-easterly (Fig. 10). Days with no snowfall typically have daily mean wind speeds below 14 m/s spread evenly between westerly to south-easterly directions. With an increasing amount of fresh snow (Fig. 10b, c, d) the distribution of wind directions gets narrower and more focused on westerly winds. Furthermore, the wind speed increases for days with more snowfall. Although it should be noted that the number of values decreases with higher snowfall, there is a clear connection between wind speed and direction to snow accumulation. As Norway is situated in the mid-latitudes westerlies, the weather is characterised by cyclones from the Atlantic Ocean. Therefore, strong westerly wind and precipitation caused by frontal passages often occur simultaneously and with the same root cause, which is well represented by the snow depth difference and wind data (Fig. 10). Additionally, the erosion or deposition of blowing snow can have influenced this result, because blowing snow only takes place during strong wind and often during precipitation. Most likely, erosion due to blowing snow is the key reason why the overall snowfall values are low.

The close relation between snow accumulation and wind direction is particularly clear for individual winter seasons. The winter seasons (from December to April and referenced by the year at the end of the winter season) of 2011, 2012, 2015, 2017, 2019, 2020 and 2022 stand out with noticeably dominant westerly winds and only rare occurrences of southerly to south-easterly winds (Fig. S6). All other winters had high occurrences of southerly to south-easterly winds. From the west, Juvfonne is sheltered by a round mountain ridge (Fig. 1a) that could lead to accumulation of wind blown snow onto Juvfonne on its lee side, but Juvfonne is facing eastward and is therefore little sheltered from the south-easterly winds. In line with this, the snow depth at the mass balance stake was higher than the trend of 13 years in 2011, 2012, 2015, 2017, 2018, 2020 and 2022 (Fig. S5) and consistently high across all Juvfonne (Fig. S3). Only 2018 with much snow and south-easterly winds and 2019 with dominant westerly winds but no snow are exceptions. This shows that year to year variations in

https://doi.org/10.5194/egusphere-2026-3152
Preprint. Discussion started: 29 June 2026

wind conditions can have significant influence on snow accumulation on Juvfonne and that westerly winds are particularly relevant for snow accumulation.

4.6 Climate conditions and development at Juvvasshøe

Mean annual precipitation (1991-2020) for the grid cell containing Juvfonne is 746 ± 21 mm, according to seNorge_2018, aligning well with previous estimates of 800–1000 mm (Østrem et al., 1988; Isaksen et al., 2011). Precipitation obtained from seNorge_2018 and observed at nearby Bøverdal station is evenly distributed throughout the year, with the lowest amounts in April and May, and the highest in January and November. Data from the snow depth sensor near Juvfonne (Fig. 1a) show that annual maximum snow depths vary between 70 and 140 cm (Fig. S5). Snow cover typically lasts from late September until early July.

The temperature data from Juvvasshøe (1894 m a.s.l.) reveal a mean annual air temperature of -3.5 °C over the period 2000-2023. Daily mean temperatures range between -20 °C and 10 °C, with monthly averages only exceeding 0 °C from June to September in this period. Over 75% of the years show negative monthly temperatures in May, but this month marks the start of the melt season with intense incoming shortwave radiation (Fig. S7) and occasional positive daytime temperatures. In contrast, nearly all days in October are below freezing, making September the last month with significant melting. By this time, Juvfonne typically reaches its annual minimum extent (Fig. 5), and the surrounding terrain has the least snow cover. Over the period of observations at Juvasshøe since 2000, we see an increase in the length of the melt season of ~5 days per decade based on days with mean temperature >0 °C (Fig. S8). Incoming shortwave (solar) radiation is the dominant contribution to the surface energy balance during the day. On Juvvasshøe its annual cycle is asymmetrical and peaks in early June (Fig. S7)

The annual variations in air temperature is illustrated by the cumulative positive degree days (CPDD). Over the period of mass balance measurements, 2010 to 2025, CPDD patterns consistently show rapid increases from May to October, with significant interannual variability (Fig. 11). The year with the highest CPDD is 2018, followed by 2024, 2021, 2014 and 2025, and the year with the lowest CPDD is 2012, followed by 2017, 2015 and 2010. Years with the highest CPDD, such as 2018, display extended periods of above-freezing temperatures, while low-CPDD years like 2012 and 2015 show delayed warming early in the melt season. The comparison of two decades (2001–2010 vs. 2011–2020) reveals an approximate 1.5% increase in CPDD values, predominantly in late spring and early autumn. The correlation (coefficient of determination) with point mass balance b_s and b_a at stake 2 are -0.56 (0.32) and -0.41 (0.17), respectively. Thus, CPDD is correlated with the point mass balance data but does not explain the variability in the point mass balance alone. As example, the year with lowest b_w, 2010, is also the year with the most negative b_a and b_s, despite having a low CPDD sum compared to other years (Fig. 11). The year with the second lowest b_s, 2016, has a higher CPDD sum than 2010, but ends up with a lower b_s and b_a.

https://doi.org/10.5194/egusphere-2026-3152
Preprint. Discussion started: 29 June 2026

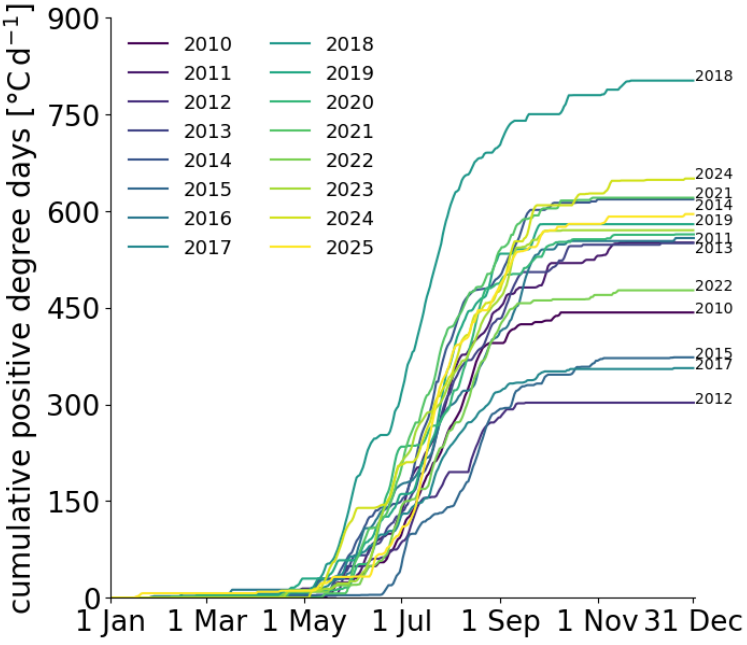

Figure 11: Cumulative positive degree days of the years 2010 to 2025. See Fig. S9 for all years 2000 to 2025.

Analysis of the cumulative Summer Melt Potential Index for summer season (May-September) at Juvvasshøe reveals an amplification of melt-inducing atmospheric conditions between 2010 and 2025 (Fig. S10). Over this 16-year observation period, the exhibits a consistent positive trend ($p = 0.086$). Concurrently, the frequency of significant melt days (defined as days exceeding the 75th percentile of the daily index distribution) has increased at a robust rate of nearly one additional day per year (+0.76 days yr^{-1}, $p = 0.114$, Fig. S10). Comparison with point mass balance measurements at stake 2 on the Juvfonne ice patch (2010-2025) physically validates this atmospheric index. The Summer Melt Potential Index exhibits a strong negative correlation with the observed summer balance (b_s, $r = -0.56$, $r^2 = 0.32$), confirming that seasons with elevated melt energy result in pronounced ice loss. Despite this underlying multi-decadal warming signal, the time series is characterized by substantial interannual variability. Distinct peak ablation seasons occurred in 2011, 2018, 2023, and 2024. However, a breakdown of the atmospheric drivers during significant melt days reveals fundamentally different ablation regimes. The year with highest CPPD, 2018, was characterized by intense radiation and sensible heat flux; a result of an exceptionally warm and dry period across southern Norway that persisted from May through early August leading to the largest summer balance recorded of nearby Storbreen and Gråsubreen glaciers (Kjøllmoen et al., 2019). This period recorded the highest daily mean air temperatures (seasonal mean of 7.9°C, with peak daily values reaching 13.8°C at 1894 m a.s.l. combined with low relative humidity (seasonal mean 74%). Conversely, the mass loss in 2011 was driven predominantly by latent heat exchanges. Despite having the lowest mean air temperature among these extreme years (6.4°C), 2011 experienced the most vigorous wind forcing (seasonal mean wind speed >8.2 m s^{-1}) and high moisture levels (seasonal mean RH 87%), triggering high condensation-driven melt. More recent extremes, notably 2023 and 2024, represent compounding events

https://doi.org/10.5194/egusphere-2026-3152
Preprint. Discussion started: 29 June 2026

where elevated air temperatures (seasonal means of 7.2°C and 7.5°C, respectively) aligned with sustained high wind speeds and high atmospheric humidity, effectively allowing both sensible and latent heat fluxes to simultaneously amplify ice ablation. Notably, 2011 recorded the absolute highest frequency of significant melt events (38 days), while 2023 similarly emerged as a highly anomalous season (28 days), underscoring a recent clustering of high-intensity melt summers.

Webcam imagery from the Galdhøpiggen summer ski centre (Fig. S4) and Sentinel-2 satellite images for Juvfonne (not shown) confirm that summer snowfalls occur. Time series of albedo calculated from Juvasshøe shortwave radiation data further demonstrate annual variability in these snowfall events (Fig. S11). In 2018, a year of high ablation, there was only one summer snowfall event that interrupted the melting period. The scarce summer snowfall combined with heavy rainfall prolonged the melting period. In contrast, multiple summer snowfalls in 2020 significantly delayed ablation. The snow depth data also revealed that the snow free period started nearly one month earlier in 2018 than 2020.

To assess the climate development for a longer time period we analysed data from the most relevant and nearby weather stations in the area (Fig. 12). Results show that the average temperature in the summer months (May-Sep) has increased significantly since the 1990s (Fig. 12a). The two temperature stations used to show the long-term trend are well correlated with the main station at Juvvasshøe (Fig. 12b) and thus should provide a representative picture of the changes at Juvfonne. Coefficient of determination (R^2) is 0.93 and 0.96 for Fokstugu-Juvvasshøe and Dombås-Juvvasshøe, respectively. For the last 40 years, 1984-2023, warming rates have been 0.39 °C per decade for both Fokstugu and Dombås weather stations. The summer of 2018 was the warmest recorded followed by 2002 and 2006. Comparable warm years were also noted in 1947 and 1901; however, when viewed over a 10-year period or longer, the recent decades are significantly warmer than those observed in the previous 150 years (Fig. 12a). The summer temperature for the recent 30-year period from 1991 to 2020 is 0.6 degrees higher in comparison to the preceding 30-year period from 1961 to 1990 for both Fokstugu and Dombås.

The amount of water vapour in the air is also increasing (Fig. 12d) for the summer season (May-Sep). For the 40-year period 1984-2023 linear trend giving an increase of 0.21 g kg^{-1} per decade. The years 2023, 2020 and 2018 are the most humid summers over the last 40 years.

Winter precipitation (Oct-Apr) has also increased significantly since the 1960s (Fig. 12c). On a decadal scale, the last 10-20 years stand out. The last 30-year period 1991-2020 has 11% more precipitation than the previous 30-year period. For the measurement period 2010-2023, prior to snow redistribution in 2024 and 2025 at Juvfonne, winter precipitation is 21% greater than 1961-1990.

https://doi.org/10.5194/egusphere-2026-3152
Preprint. Discussion started: 29 June 2026

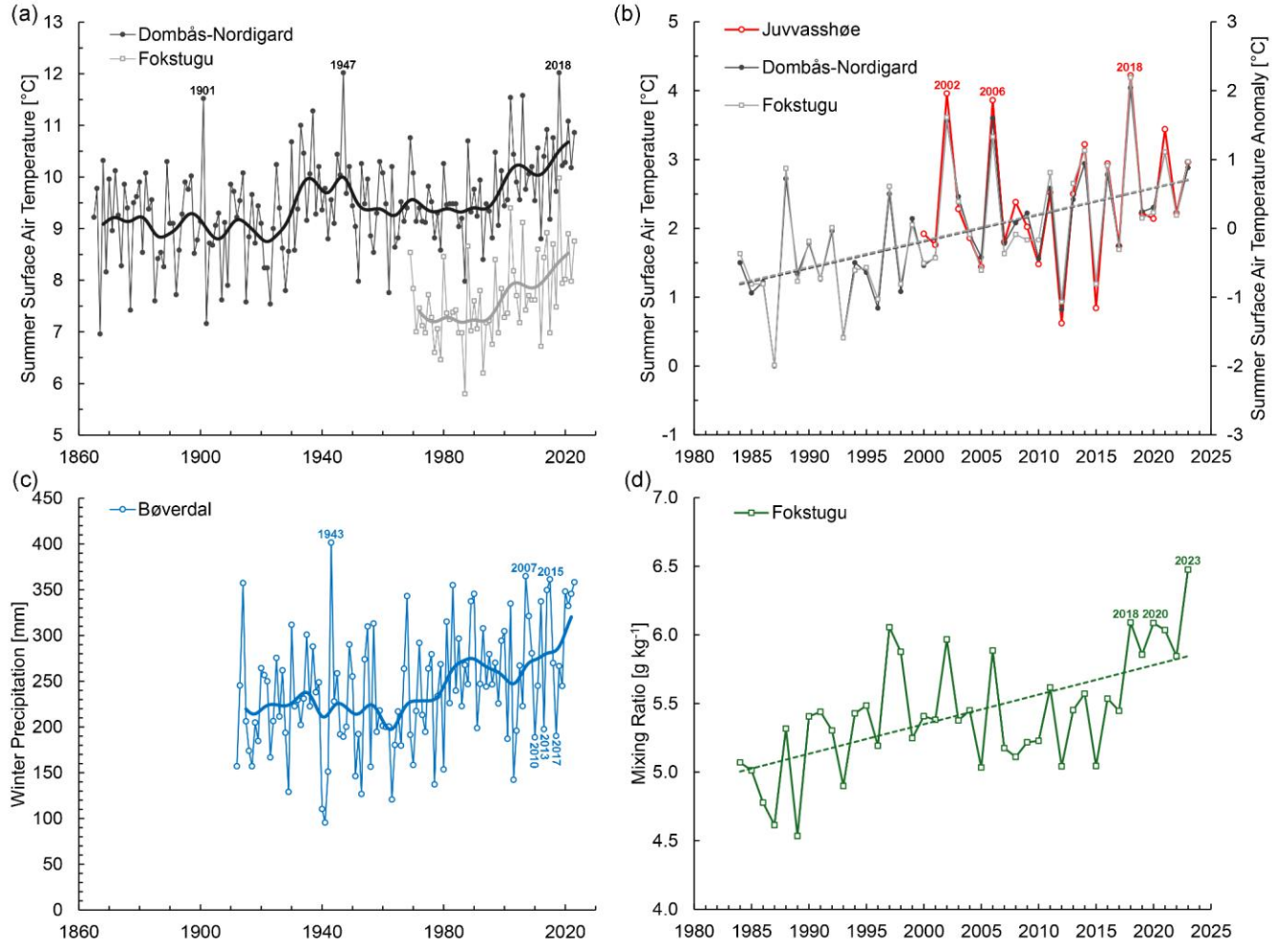

Figure 12: Climate development for key parameters important for melting in the summer and accumulation in the winter. (a) The mean temperature for the summer season (May, June, July, August and September) at the weather stations Dombås-Nordigard and Fokstugu. The thick line shows the temperature development smoothed on an approximately 10-year scale. (b) Same as in (a), but for the latest 40-year period 1984-2023 and where the actual summer season temperature at Juvvasshøe (red curve, 2000-2023) is compared with the deviation from the normal (1991-2020) for the other two stations (second y-axis). Linear trend is shown for the 40-year period for Dombås-Nordigard and Fokstugu (c) Winter precipitation (Oct-Apr) observed at Bøverdal station. The thick line shows the precipitation development smoothed on an approximately 10-year scale. (d) The amount of water vapour in the air, shown as mixing ratio, i.e. the ratio of the mass of water vapour to mass of dry air calculated based on observations at Fokstugu for the summer season (May-Sep) for the 40-year period 1984-2023. Linear trend is shown, giving an increase of 0.21 g kg-1 per decade. The three most significant record years are denoted by the year labels on each of the figures. Also noted in (c) are the three winters with the least precipitation during the mass balance period (2010-2023), which were marked as the final year in the period from October to April.

https://doi.org/10.5194/egusphere-2026-3152
Preprint. Discussion started: 29 June 2026

4.7 Comparison with other glaciers and ice patches in Jotunheimen

To assess how the changes of Juvfonne are compared to other ice bodies in the region, we assessed the repeat lidar surveys covering Juvfonne and the Galdhøpiggen massif over the period 2011-2020 (Fig. 13). Juvfonne is the northernmost of the 19 compared ice bodies (Fig. 13, Table 1). Except for the two smallest units (ID 2602 and ID 2617) that had a slight thickening amounting to 0.7-0.8 ± 0.02 m a^{-1}, all glaciers have thinned over the period 2010-2020. The thinning varies from −0.19 ± 0.02 m a^{-1} on Juvfonne to −2.07 ± 0.02 m a^{-1} for Kjelen. The large thinning of the small cirque glacier Kjelen can probably partly be attributed to calving. Kjelen is the only one of the studied glaciers that has a proglacial lake and where lake calving plays a role. Additional warming from the dark cirque walls surrounding the glacier as the snow and ice has vanished may also have intensified the melting. Juvfonne has built up a surplus in upper parts and so have some of the other glaciers. All glaciers have shrunk in their lower parts. The difference maps also indicate some thickening in the uppermost parts of the glaciers, which is also remarked for Juvfonne (Fig. 13). It should be noted that the period covered by the laser scanning from 17 September 2011 to 18 August 2020 does not include the first two years (2009/2010 and 2010/2011) with high mass deficit measured at Juvfonne (Fig. 3). Moreover, the mean thinning for Juvfonne over 2011-2020 is smaller than observed for the 2011-2019 period (Sect. 4.3) due to thickening and snow remaining at in 2020.

The area of Juvfonne shrunk by 32% from 2011 to 2019 (8 years) using the outline digitised from the 2019 orthophoto. In total the 19 glaciers studied shrunk from 35.9 km^2 to 34.6 km^2 over the 8-year period, an area reduction of 4%. The glaciers in the Galdhøpiggen massif were also mapped by a Landsat image from 9 August 2003 in the previous national glacier inventory (Andreassen et al., 2008a; Andreassen et al., 2012). The 19 glaciers there had a total area of 36.9 km^2. The reduction from 2003 to 2019 is thus 6%. Juvfonne had an area of 0.15 km^2 in the 9 August 2003 Landsat image and 0.11 km^2 in 2019 derived from the 4 August Sentinel-2 image, a reduction in area of 30%. Results from two other smaller nearby glaciers with multiple archaeological finds, Storbreen (ID1723) and Lendbreen (ID 2541), show an even stronger area reduction from 2003 to 2019 (Andreassen et al., 2020). Storbreen reduced from 0.0154 km^2 to 0.0985 km^2 (82%) and Lendbreen from 0.429 to 0.175 km^2 (145%).

The findings point to large changes of the smaller glaciers and ice patches. As noted by Andreassen et al. (2022) smaller glaciers and ice patches such as Juvfonne can have large percentage area variations due to melting around the perimeter through the season and will also be more sensitive to the spatial resolution of the sensor used to map the glacier outline. We also see in our detailed and high-resolution mapping of the glacier outline of Juvfonne how it can vary depending on the snow conditions the previous year(s) and of timing in summer (Fig. 2, 5). Although there will be more uncertainties in mapping smaller entities using medium resolution satellite images than orthophotos and one must take care when assessing outlines, our accurate mapping of the glacier outlines of Juvfonne show a clear and large reduction in area over the observation period.

https://doi.org/10.5194/egusphere-2026-3152
Preprint. Discussion started: 29 June 2026

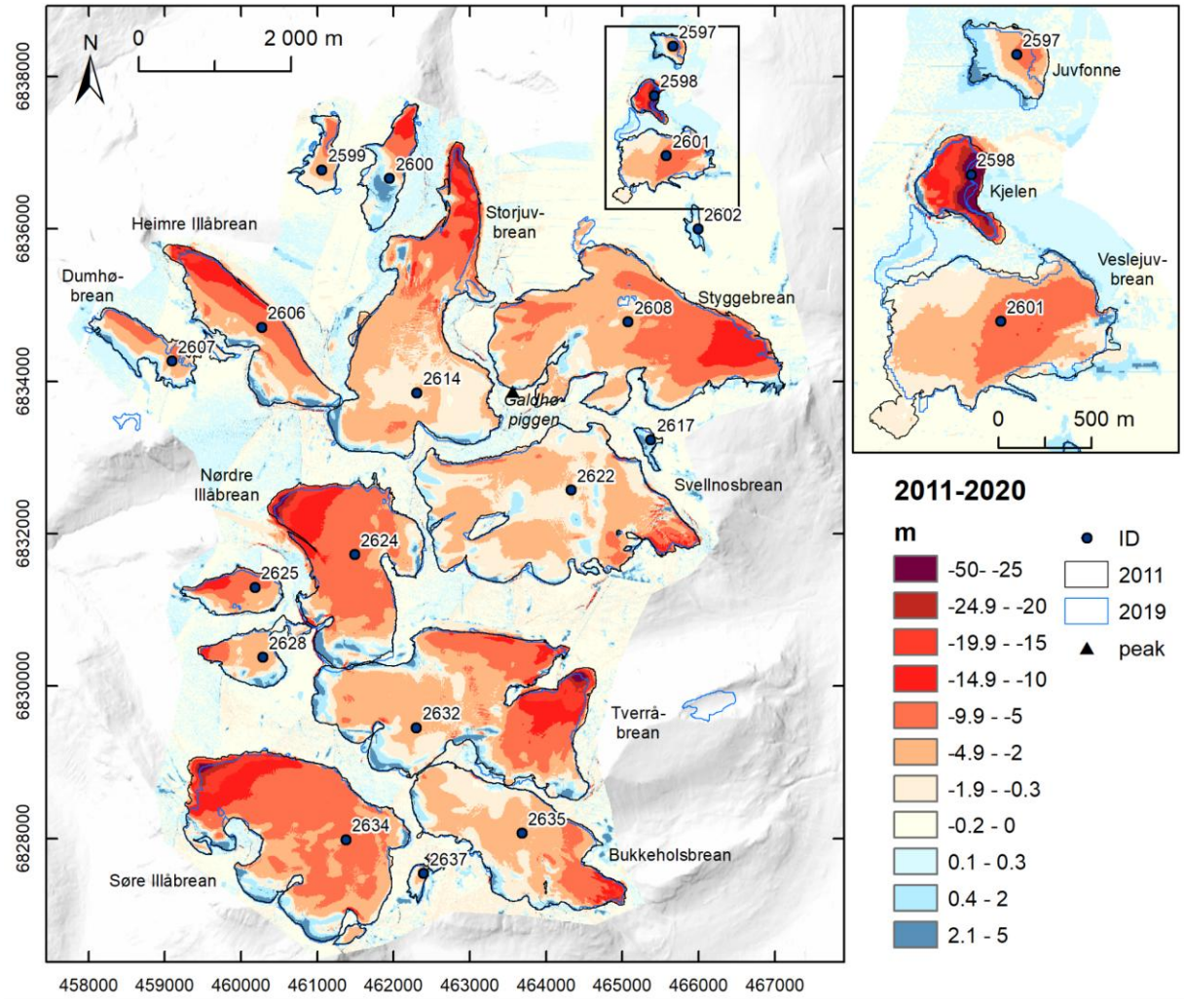

Figure 13: Elevation change from repeat laser scanning in 2011 and 2020 for glacier in the Galdhøpiggen (Norway's highest peak) massif. The inset details Juvfonne, Kjelen and Vesljuvbrean. Background hillshade from Norwegian mapping authority. Coordinate system UTM 32N.

Table 1: Results of DTM differencing of Juvfonne and 18 other glaciers in the Galhøpiggen massif. See Figure 13. Date 1: date of lidar and aerial photos (ap) first survey, Date 2 (lidar): date of lidar second survey. Date 2 (ap or S2): date of outline from orthophotos of 26 August 2019 for Juvfonne (2597) and Kjelen (2598) and Sentinel-2 (S2) orthoimage (other glaciers) from 4 or 27 August 2019.

ID	Name	Date1 (lidar +ap)	Date2 (lidar)	Area1 (km^2)	Area2 (km^2)	dA (km^2)	dA (%)	Date2 (ap or S2)	dh (m)	dh (m a^{-1})
2597	Juvfonne	17.09.2011	18.08.2020	0.13	0.09	0.04	31.9	26.08.2019	-1.70	-0.19
2598	Kjelen	17.09.2011	18.08.2020	0.15	0.10	0.05	31.8	26.08.2019	-18.65	-2.07
2599		17.09.2011	18.08.2020	0.33	0.33	0.00	-0.1	04.08.2019	-2.43	-0.27
2600	Storgrovbrean	17.09.2011	18.08.2020	0.64	0.63	0.01	1.5	04.08.2019	-2.62	-0.29
2601	Vesljuvbrean	17.09.2011	18.08.2020	0.76	0.73	0.02	3.3	04.08.2019	-3.32	-0.37

https://doi.org/10.5194/egusphere-2026-3152
Preprint. Discussion started: 29 June 2026

2602		17.09.2011	18.08.2020	0.07	0.06	0.02	20.5	04.08.2019	0.74	0.08
2606	Heimre Illåbrean	17.09.2011	18.08.2020	1.72	1.65	0.07	4.1	04.08.2019	-5.15	-0.57
2607	Dumhøbrean	17.09.2011	18.08.2020	0.72	0.58	0.14	19.8	04.08.2019	-2.33	-0.26
2608	Styggebrean	17.09.2011	18.08.2020	4.91	4.83	0.08	1.6	04.08.2019	-4.61	-0.51
2614	Storjuvbrean	17.09.2011	18.08.2020	4.52	4.34	0.18	4.0	04.08.2019	-3.68	-0.41
2617		17.09.2011	18.08.2020	0.08	0.07	0.01	14.0	27.08.2019	0.86	0.10
2622	Svellnosbrean	17.09.2011	18.08.2020	4.91	4.85	0.06	1.2	27.08.2019	-2.23	-0.25
2624	Nørdre Illåbrean	17.09.2011	18.08.2020	3.05	2.97	0.08	2.6	27.08.2019	-6.54	-0.73
2625		17.09.2011	18.08.2020	0.55	0.50	0.04	7.9	27.08.2019	-5.25	-0.58
2628		17.09.2011	18.08.2020	0.62	0.52	0.10	16.5	04.08.2019	-2.57	-0.29
2632	Tverråbrean	17.09.2011	15.08.2020	5.18	5.12	0.06	1.2	27.08.2019	-4.42	-0.49
2634	Søre Illåbreen	17.09.2011	15.08.2020	4.54	4.33	0.22	4.8	04.08.2019	-5.90	-0.66
2635	Bukkeholsbrean	17.09.2011	15.08.2020	2.84	2.80	0.04	1.5	27.08.2019	-2.94	-0.33
2637		17.09.2011	15.08.2020	0.13	0.08	0.05	39.2	27.08.2019	-1.95	-0.22
19				**35.86**	**34.58**	**1.27**	**-3.5**		**-4.22**	**-0.47**

5 Discussion

5.1 Mass balance drivers of Juvfonne

Snow plays a pivotal role in the mass balance dynamics of Juvfonne. The sheltered topography of the ice patch enhances snow retention, while wind-driven redistribution contributes to localized variations in accumulation. Significant snowfall events, particularly those associated with westerly storms, are crucial in replenishing the ice patch, offsetting melt losses during warmer seasons. However, the shorter snow season and increasing temperature poses a growing challenge to its ability to maintain mass. These processes underline the importance of understanding not only annual precipitation totals but also the spatial and temporal variability of snow deposition in shaping the ice patch's behaviour. Summer precipitation also influences melting. Summer snowfall protects glaciers by increasing albedo, insulating ice, and cooling the surface during melt (Oerlemans and Klok, 2004). We also found this in the data collected for Juvvasshøe, but we cannot determine any trend over Juvfonne over the observation period. However, higher summer temperatures will likely reduce the number of summer snow falls in the future. Previous studies of the energy balance at the nearby Storbreen glacier have shown that variations in temperature and reflected shortwave radiation (albedo) explain most of the interannual variation in melt (Andreassen et al., 2008b), whereas studies of ice patches in the Canadian High Arctic reveal that the short-term variability in melt rate is driven by sensible heat fluxes (Davesne et al., 2023). Moreover, a comparison of the Storbreen and Midtdalsbreen glaciers, 120 km apart, finds that the importance of net radiation decreases over the melt season, while the turbulent fluxes become more important (Giesen et al., 2009). Results from Juvvasshøe reveal that incoming shortwave (solar) radiation is the dominant contribution to the surface energy balance during the day and its annual cycle peaks in early June (Fig. S7), similar to

https://doi.org/10.5194/egusphere-2026-3152
Preprint. Discussion started: 29 June 2026

observations and analysis of long-term energy balance trends in permafrost sites in the Swiss Alps (Hoelzle et al., 2022). While strong radiation in spring and early summer can initiate early melting, its impact depends on surface albedo and nighttime refreezing. Lower albedo of wet or dirty snow in spring amplifies the effect of shortwave radiation, particularly when temperatures remain above freezing overnight. Depending on the cloud fraction, cloud base temperature and water vapor content of the atmosphere, longwave (thermal) radiation can have either a warming or cooling effect on the ice patch. Sensible and latent turbulent heat fluxes complete the surface energy balance but are not measured at Juvfonne. These fluxes are also particularly difficult to characterize due to theoretical constraints of turbulence in complex terrain and interactions of large-scale, valley and slope winds (Sauter et al., 2026). The horizontal advection of heat can induce strong downward sensible heat fluxes at glacier margins. We expect this to be particularly relevant for Juvfonne, because of its small size. Latent heat fluxes and moisture transport have become more important for Juvfonne, as the humidity has increased significantly over the last decades during summer (Fig. 12). Condensation of water vapor on the snow during warm, moist air intrusions transfer latent heat to the snow, further increasing melt. Furthermore, strong wind and low humidity can cause strong surface sublimation and sublimation of blowing snow which reduces the mass balance (Mott et al., 2018), even at temperatures below freezing.

The comparison of the CPDD calculated from the air temperature data from Juvvasshøe and the point mass balance at Juvfonne revealed correlations between CPDD and summer and annual balance, although variations in CPDD alone does not explain the variance in melting. It should be noted that CPDD does not account for nighttime refreezing, crucial for possible refreezing of melt water.

5.2 Glacier-ice patch transition in a permafrost environment

To separate glaciers from perennial snow fields and smaller ice bodies a glacier is defined as 'A perennial mass of ice, and possibly firn and snow, originating on the land surface by the recrystallization of snow or other forms of solid precipitation and showing evidence of past or present flow' in the UNESCO/IACS mass balance glossary (Cogley et al., 2011). According to this definition it is not required to have present flow to be a glacier. When glaciers shrink, they may transit into small stagnant ice bodies. A glacieret is defined as 'A very small glacier, typically less than 0.25 km^2 in extent, with no marked flow pattern visible at the surface. To qualify as a glacieret, an ice body must persist for at least two consecutive years. 'Glacierets can be of any shape, and usually occupy sheltered parts of the landscape. Windborne snow and avalanches can be dominant contributors to the accumulation of glacierets' (Cogley et al., 2011). The term ice patch is not defined in Cogley and others (2011). In a collection of nearly 30 papers describing vanishing glaciers, it was found that ice patches were a more commonly used term than glacierets (Andreassen et al., 2026). The term very small glaciers is also used in the literature, with varying size definitions as glaciers of size < 0.1 km^2 (Kuhn, 1995) and < 0.5 km^2 (Huss, 2010). We have used the term ice patch for Juvfonne meaning a glacier or ice body currently too small to have any notable flow, but according to the definitions by Cogley et al. (2011) Juvfonne is likely also a glacier with evidence of past flow. It could also be categorised as a glacieret with its current size, lack of crevasses and no significant current flow.

https://doi.org/10.5194/egusphere-2026-3152
Preprint. Discussion started: 29 June 2026

The basal ice of Juvfonne has been dated to be over 7000 years old, demonstrating that the ice patch has persisted over a long time span (Ødegård et al., 2017), including through parts of the Holocene Thermal Maximum (HTM). The preservation of small ice patches like Juvfonne during warmer climatic periods is closely linked to two primary factors: (1) the ground thermal regime of the underlying permafrost, and (2) the magnitude of winter snowdrift, which acts to balance high summer ablation.

Concerning (1), permafrost has likely existed at the elevation of Juvfonne during all the Holocene, even through the HTM (Lilleøren et al. 2012), and serving as a key stabilizing factor. As long as the ice-patch persists, permafrost is preserved underneath because summer ground surface temperatures never exceed 0 °C, while winter cold can still penetrate the ice body (e.g. Ballantyne, 1978)., particularly when accounting for three-dimensional effects. Consequently, the suppression of subsurface melting significantly enhances the longevity of ice patches. However, recent studies (e.g., Isaksen et al., 2022; Etzelmüller et al., 2023) and updated regional monitoring data (cryo.met.no/permafrost) reveal a significant warming trend in permafrost temperatures alongside a deepening of the active layer within this area. While this warming will undoubtedly influence summer melt (see below), it does not immediately alter the thermal regime at the base of the ice patch, thereby temporarily delaying the basal decay process. Juvfonne likely developed its initial ice-layers during a post-deglaciation period when the climate was warmer or similar to today (i.e., during the HTM). The presence of permafrost then (e.g. Lilleøren et al., 2012) facilitated the preservation of these early ice layers, which subsequently built up during the cooling phase following the HTM. Thus, a feedback loop exists: the underlying permafrost delays the degradation of the ice patch, while the ice patch concurrently prevents the degradation of permafrost in its immediate vicinity during periods of climate change.

Concerning (2), Juvfonne has had a larger extent historically with an estimated area of 0.288 km^2 at its LIA maximum extent (Baumann et al., 2009) and maximum thickness of 40-50 m (Nesje et al., 2011). We revisited the LIA extent and found it difficult to determine the exact shape due to lack of end moraines but estimated a LIA area of about 0.311 to 0.629 km^2 from orthophotos from 2024 (Fig. S12). Juvfonne has no visible moraines from orthophotos, the lack of moraines has also been observed in the field (Atle Nesje, personal communication February 2026). From the orthophotos the maximum extent can be drawn from the bleached parts in the landscape, much of this may be due to persistent snowfields. However, it is likely that Juvfonne was thicker and could deform at its maximum extent in the 18th century. The first years of mass balance measurements showed a strong decrease in surface elevation, but then several years of positive mass surplus followed. The ice patch is obviously dependent on and survives due to snow accumulation and topographic effects similar to other ice patches (e.g. Arie et al., 2025). Our observations and analyses demonstrate that episodic, high-magnitude windblown snowfall events can contribute disproportionately to the total accumulation. Despite a long-term deficit, Juvfonne retains the capacity for transient mass gain, as exemplified by the growth of the western parts between 2015 and 2018. However, in other years, such as the melt season of 2019, the ice patch becomes entirely free of the snow and firn from recent years. Under such conditions, the mass surplus from previous years is effectively eliminated, preventing the formation of a firn reservoir over time that later

https://doi.org/10.5194/egusphere-2026-3152
Preprint. Discussion started: 29 June 2026

could have built up new ice through firn to ice transformations (e.g. Kawashima et al., 1993). The removal of the protective, high-albedo snow and firn cover exposes older ice with higher concentrations of dust and organic impurities; this triggers a positive albedo feedback that further enhances energy absorption and accelerates the ablation process. Despite annual fluctuations in the extent of Juvfonne, our results reveal a substantial shrinking in area of over 46% from 2010 to 2024. The volume loss is even more striking, with an estimated reduction of 73% of the ice patch between 2011 and 2025.

Although part of Juvfonne has survived the last millennium, current global warming threatens its continued existence (cf. Ødegård et al., 2017). The global warming seen from 1970 to 2020 is unprecedented; it is likely faster than any other 50-year period within the last 2000 years due to anthropogenic climate change (Paasche et al., 2025). This global signal is clearly reflected in the local records from Fokstugu and Dombås - Nordigard, which show a significant warming trend consistent with the national average of approximately 1.3 °C since 1900 (Tajet et al., 2025). Looking ahead, climate projections indicate that this trend will intensify. The future warming predicted for the remaining 75 years until 2100 suggests an increase in mean summer temperatures of 2-4 °C for the southern mountain areas in Norway, depending on the emission scenario (Dyrrdal et al., 2025). For a high-elevation site like Juvfonne, such a trajectory implies a drastic increase in days with summer melting and frequency of years with complete snow removal. (cf. Dyrrdal et al., 2025). The current remaining ice thickness of 2-4 m over larger parts, with a maximum of less than 9 meters, means that Juvfonne may lose its last ice within a decade or two. A combination of several consecutive years with low winter accumulation and warm summers may accelerate this process. When ice patches lose their last ice, they may retain the capacity to accumulate seasonal snow, firn, or even new ice, but archaeologically they are fundamentally altered and may be defined as a “ghost patch” (Kristensen and Andreassen, 2026).

6 Conclusions

The 16-year monitoring program (2010-2025) of Juvfonne provides a comprehensive basis for studying the dynamics and climate sensitivity of Norway’s most archaeologically and glaciologically investigated ice patch. Our findings highlight a stark and accelerating decline: Juvfonne has lost 46% of its area since 2010 and 73% of its volume since 2011, with an average surface thinning of 0.30 m a^{-1}. With a maximum ice thickness now measured at less than 9 meters and an average thickness below 3 meters, the ice patch is approaching a critical threshold where its remaining ancient ice - dating back over 7,600 years - is at risk of completely vanishing within a few exceptionally warm summers.

Our study shows that the mass balance of Juvfonne is governed by a complex interplay of topographic and atmospheric drivers:

- Juvfonne prevails primarily due to the efficient capture of wind-blown snow. Its position within a sheltered topographic depression allows it to accumulate significantly more snow than the surrounding terrain, particularly during westerly storm events. This "topographic filling" mechanism provides a degree of resilience, allowing the ice patch to partially recover during years with favourable conditions.

https://doi.org/10.5194/egusphere-2026-3152
Preprint. Discussion started: 29 June 2026

- Cumulative Positive Degree Days (CPDD) reveal an approximate 1.5% decadal increase and correlate with Juvfonne's point mass balance. However, this temperature-only index is insufficient to explain the full interannual variability on its own. Anomalous ablation seasons like 2010 and 2016 demonstrate that thermodynamic forcing alone cannot account for the diverse melting regimes. A Summer Melt Potential Index generally supports the CPDD results and reveals a significant increase in melt-inducing atmospheric conditions since 2010, with a corresponding intensification of significant melt events. These results also correlate with observed ice loss on Juvfonne and identify a shift toward 'compounding melt events' driven by a synergy of elevated temperatures, wind speeds, and atmospheric moisture. Long-term trends in temperature, precipitation and humidity in the region support the finding of a steadily warming and more humid climate.
- Compared to nearby glaciers, Juvfonne has experienced less surface thinning due to its specific topographic characteristics and favourable accumulation patterns. However, its smaller size makes it significantly more vulnerable to complete loss within a few decades, particularly under conditions of several consecutive years with low winter accumulation and warm summers.
- Despite its relative resilience compared to larger neighbouring glaciers, Juvfonne remains highly vulnerable for climate change. Several "snow-free" summers, such as observed in 2019 and 2024, removes the protective high-albedo snow cover and exposes the ancient ice core directly to solar radiation and sensible heat. Its long-term survival is severely constrained by its current thickness and volume. Further projected temperature increase and altered precipitation patterns, are likely to accelerate ice loss. The disappearance of Juvfonne would not only have glaciological implications but also threaten the archaeological materials preserved within the ice.
- Permafrost plays a critical role in stabilizing and preserving small ice patches like Juvfonne. However, observations from the area indicate significant warming and degradation of permafrost in recent decades, as documented in recent studies. This warming not only reflects the same physical processes driving ice melt - such as increased air and ground temperatures, changes in snow cover, and altered energy fluxes - but also destabilizes the frozen substrate essential for preserving small ice patches like Juvfonne. The combined effects of atmospheric warming and permafrost degradation highlight the urgency of monitoring these interconnected processes to better understand their implications for small ice patches and their broader climatic, glacial and archaeological significance.

Data availability

Meteorological data were retrieved from the Norwegian Meteorological Institute (MET Norway) via the Frost API (https://frost.met.no/) on 8 September 2025, and 16 January 2026 as well as from seklima.no downloaded 9 April 2023 and 23 May 2026. The API and seklima.no services provide free public access to MET Norway's historical weather and climate archives. Data from NORA3 were downloaded from https://data.met.no/ on 23 January 2023. Glaciological and geodetic mass balance data will be submitted to WGMS. Glacier outlines from the detailed mapping, ice thickness point data and processed

https://doi.org/10.5194/egusphere-2026-3152
Preprint. Discussion started: 29 June 2026

DTMs from the UAV surveys will be available through Nasjonalt Vitenarkiv as doi <provide doi at time of publication of preprint>. Glacier outlines from previous regional or national inventories LIA, 1981, 1997, 2003 and 2019 and detailed outline 26 August 2019 are available in the GLIMS database and GLIMS viewer: https://www.glims.org/maps/glims, other outlines 2010-2025 will be submitted to GLIMS. The orthophotos from 2011, 2017, 2019, 2023 and other images are available at https://www.norgeibilder.no/. Lidar data from 2011 and 2020 are available at https://hoydedata.no/.

Supplement link: The supplementary material is provided in a separate file which is available online.

Author contributions

LMA, KI and LMK made the figures, tables and wrote the paper with contributions from all authors. All authors contributed to data collection and data analyses and read the final manuscript.

Competing interests

The authors declare that they have no conflict of interest.

Acknowledgements

The work on Juvfonne is a contribution to 'Klimapark 2469' – a nature park and outdoor discovery centre in the alpine region around Galdhøpiggen, the highest mountain peak in Norway (2469 m a.s.l.) and contributes to the Fjellviten project. The authors thank partners in Klimapark 2469 and Dag Inge Bakke and Olav Tøfte for observations and support. The internship of LMK at NVE was funded by the Erasmus+ programme of the European Union. LMA thanks the numerous NVE colleagues that contributed to mass balance measurements over 2010-2025.

References

Andreassen, L. M.: Breer og fonner i Norge, NVE Rapport no. 3/2022, Norwegian Water Resources and Energy Directorate, https://publikasjoner.nve.no/rapport/2022/rapport2022_03.pdf, 2022.

Andreassen, L. M. and De Marco, J.: Brekartlegging med drone. NVE Rapport no. 44/2018, Norwegian Water Resources and Energy Directorate, https://publikasjoner.nve.no/rapport/2018/rapport2018_44.pdf, 2018.

https://doi.org/10.5194/egusphere-2026-3152
Preprint. Discussion started: 29 June 2026

Andreassen, L. M., Adalgeirsdottir, G., Berthier, E., Flowers, G., Hannesdottir, H., Huss, M, Menunuous, B., Paul, F.,and Ruiz, L.: Vanishing glaciers. Introduction to the Annals of Glaciology Collection, Annals of Glaciology, 67, https://doi.org/10.1017/aog.2026.10051, 2026.

Andreassen, L. M. (red.), Callanan, M., Saloranta, T. Kjøllmoen, B., and Nagy. T.: FonnSat - Fonner, arkeologi og satellittdata, NVE Rapport no. 42/2020, Norwegian Water Resources and Energy Directorate, https://publikasjoner.nve.no/rapport/2020/rapport2020_41.pdf, 2020a.

Andreassen, L. M., Paul, F., Kääb, A., and Hausberg, J. E.: Landsat-derived glacier inventory for Jotunheimen, Norway, and deduced glacier changes since the 1930s, The Cryosphere, 2, 131–145, doi:10.5194/tc-2-131-2008, 2008a.

Andreassen, L.M., Nagy, T., B. Kjøllmoen, B., and Leigh, J.R.: An inventory of Norway's glaciers and ice-marginal lakes from 2018–19 Sentinel-2 data, Journal of Glaciology, 1–22, 2, https://doi.org/10.1017/jog.2022.20, 2022.

Andreassen, L. M., Robson, B.A., Smith, M., Weber, P., Carrivick, J.L. and Kjøllmoen, B.: Tracing the rapid loss of Breifonn, Norway's southernmost glacier, Annals of Glaciology, 66, e30, https://doi.org/10.1017/aog.2025.10029, 2025.

Andreassen, L. M., van den Broeke, M. R., Giesen, R.H., and Oerlemans, J.: A five-year record of surface energy and mass balance from the ablation zone of Storbreen, Norway. Journal of Glaciology, 54 (185), 245-258, https://doi.org/10.3189/002214308784886199, 2008b.

Arie, K., Narama, C., Fukui, K. and Iida. H.: Identification and persistence mechanism of very small glaciers and perennial snow patches in the northern Japanese Alps. Front. Earth Sci. 13:1442884. doi:10.3389/feart.2025.1442884, 2025.

Ballantyne, C. K.: The Hydrologic Significance of Nivation Features in Permafrost Areas. Geografiska Annaler: Series A, Physical Geography, 60(1–2), 51–54. https://doi.org/10.1080/04353676.1978.11879963, 1978.

Baumann, S., Winkler, S., and Andreassen, L. M.: Mapping glaciers in Jotunheimen, South-Norway, during the "Little Ice Age" maximum, The Cryosphere, 3, 231–243, https://doi.org/10.5194/tc-3-231-2009, 2009.

Benestad, R. E.: Climate Change Scenarios for Northern Europe from Multi-Model IPCC AR4 Climate Simulations: DOWNSCALED MULTI-MODEL SCENARIOS'. Geophysical Research Letters 32 (17), https://doi.org/10.1029/2005GL023401, 2005.

https://doi.org/10.5194/egusphere-2026-3152
Preprint. Discussion started: 29 June 2026

Benestad, R. E, Parding, K. M., Isaksen, K. and Mezghani, A.: Climate Change and Projections for the Barents Region: What Is Expected to Change and What Will Stay the Same?' Environmental Research Letters 11 (5): 054017. https://doi.org/10.1088/1748-9326/11/5/054017, 2016.

Campbell Scientific Technical Communications: SR50A-Series. Product Manual, 2021.

Cogley, J. G., Hock, R., Rasmussen, L. A., Arendt, A. A., Bauder, A., Braithwaite, R. J., Jansson, P., Kaser, G., Möller, M., Nicholson, L., and Zemp, M.: Glossary of Glacier Mass Balance and Related Terms, IHP-VII Technical Documents in Hydrology No. 86, IACS Contribution No. 2, Paris, UNESCO-IHP, 114 pp., 2011.

Davesne, G., Fortier, D., Domine, F., Kinnard. C.: Mass-balance and ablation processes of a perennial polar ice patch on the northern coast of Ellesmere Island. Journal of Glaciology 69(278), 1598–1615. https://doi.org/10.1017/jog.2023.44, 2023.

De Marco, J., Carturan, L., Maset, E., Cucchiaro, S., Visintini, D., De Infanti, R., and Cazorzi, F.: Century-long multi-source analyses highlight decreasing vulnerability for a small, debris-covered and avalanche-fed glacier in the eastern Italian Alps. Journal of Hydrology, 615, Part A, 128586, https://doi.org/10.1016/j.jhydrol.2022.128586, 2022

Dyrrdal, A.V., Bakke, S.J., Hanssen-Bauer, I., Mayer, S., Nilsen, I.B., Nilsen, J.E.Ø., Paasche, Ø., Saloranta, T., and Årthun, M. [editors]: Klima i Norge – kunnskapsgrunnlag for klimatilpasning oppdatert i 2025, NCCS-rapport 1/2025, https://doi.org/10.60839/4rgq-nn84, 2025.

Etzelmüller, B., Isaksen, K., Czekirda, J., Westermann, S., Hilbich, C., and Hauck, C.: Rapid warming and degradation of mountain permafrost in Norway and Iceland, The Cryosphere, 17, 5477–5497, https://doi.org/10.5194/tc-17-5477-2023, 2023.

Farbrot, H., Hipp, T. F., Etzelmuller, B., Isaksen, K., Odegard, R. S., Schuler, T. V., and Humlum, O.: Air and Ground Temperature Variations Observed along Elevation and Continentality Gradients in Southern Norway, Permafrost Periglac., 22, 343–360, https://doi.org/10.1002/ppp.733, 2011.

Finstad, E., Martinsen, J., Hole, R., and Pilø, L.: Prehistoric and medieval skis from glaciers and ice patches in Norway. Journal of Glacial Archaeology 3: 43–58, https://doi.org/10.1558/jga.33147, 2018.

Fujita, K., Hiyama, K., Iida, H. and Ageta, Y.: Self-regulated fluctuations in the ablation of a snow patch over four decades, Water Resour. Res., 46, W11541, doi:10.1029/2009WR008383, 2010.

https://doi.org/10.5194/egusphere-2026-3152
Preprint. Discussion started: 29 June 2026

Getis, A. and Ord, J.K.: The Analysis of Spatial Association by Use of Distance Statistics. Geographical Analysis, 24, 189-206, https://doi.org/10.1111/j.1538-4632.1992.tb00261.x, 1992

Gillespie, M. K., Andreassen, L. M., Huss, M., de Villiers, S., Sjursen, K. H., Aasen, J., Bakke, J., Cederstrøm, J. M., Elvehøy, H., Kjøllmoen, B., Loe, E., Meland, M., Melvold, K., Nerhus, S. D., Røthe, T. O., Støren, E. W. N., Øst, K., and Yde, J. C.: Ice thickness and bed topography of Jostedalsbreen ice cap, Norway. Earth System Science Data, 16(12), 5799–5825. https://doi.org/10.5194/essd-16-5799-2024, 2024.

Haakenstad, H. and Ø. Breivik. NORA3. Part II: Precipitation and Temperature Statistics in Complex Terrain Modeled with a Nonhydrostatic Model. J. Appl. Meteor. Climatol., 61, 1549–1572, https://doi.org/10.1175/JAMC-D-22-0005.1, 2022.

Haeberli, W., Frauenfelder, R., Kääb, A., and Wagner, S.: Characteristics and potential climatic significance of "miniature ice caps" (crest- and cornice-type low-altitude ice archives), J. Glaciol., 50, 129–136, doi:10.3189/172756504781830330, 2004.

Hipp, T., Etzelmüller, B., Farbrot, H., Schuler, T. V., and Westermann, S.: Modelling borehole temperatures in Southern Norway – insights into permafrost dynamics during the 20th and 21st century, The Cryosphere, 6, 553–571, https://doi.org/10.5194/tc-6-553-2012, 2012.

Hock, R.: Glacier melt: a review of processes and their modelling. Progress in physical geography, 29(3), 362-391, 2005.

Hoelzle, M., Hauck, C., Mathys, T., Noetzli, J., Pellet, C., and Scherler, M.: Long-term energy balance measurements at three different mountain permafrost sites in the Swiss Alps. Earth System Science Data, 14(4), 1531-1547, 2022.

Huss, M.: Massbalance of Pizolgletscher. Geogr.Helv. 64, 80–92, doi:10.5194/gh-65-80-2010, 2010.

Isaksen, K., Heggem, E., Bakkehøi, S., Ødegård, R., Eiken, T., Etzelmüller, B., and Sollid, J.: Mountain permafrost and energy balance on Juvvasshøe, southern Norway. In Proceedings Volume 1, Eight International Conference on Permafrost, Zurich, Switzerland, 21-25 July, Phillips M, Springmann SM, Arenson LU (eds.). Swets & Zeitlinger, Lisse, ISBN 9058095827: 467–472. doi:10.13140/2.1.1319.9040, 2003.

https://doi.org/10.5194/egusphere-2026-3152
Preprint. Discussion started: 29 June 2026

Isaksen, K., Lutz, J., Sørensen, A., Godøy, Ø., Ferrighi, L., Eastwood, S., Aaboe, S.: Advances in operational permafrost monitoring on Svalbard and in Norway. Environmental Research Letters 17 095012, https://doi.org/10.1088/1748-9326/ac8e1c, 2022.

Isaksen, K., Ødegård, R. S., Etzelmüller, B., Hilbich, C., Hauck, C., Farbrot, H., Eiken, T., Hygen, H. O., Hipp, T.F.:. Degrading mountain permafrost in southern Norway - spatial and temporal variability of mean ground temperatures 1999-2009. Permafrost Periglacial Processes. DOI: 10.1002/ppp.728, 2011.

Kawashima, K, Yamada, T., Wakahama, G.: Investigations of internal structure and transformational processes from firn to ice in a perennial snow patch, Annals of Glaciology, 18:117-122, doi:10.3189/S0260305500011368 1993, 1993.

Kjøllmoen, B. (Ed.), Andreassen, L.M., Elvehøy, H., Jackson, M., Giesen, R.H.: Glaciological investigations in Norway in 2010. NVE Report no. 3/2011, Norwegian Water Resources and Energy Directorate, https://publikasjoner.nve.no/report/2011/report2011_03.pdf, 2011.

Kjøllmoen, B. (Ed.), Andreassen, L.M., Elvehøy, H., Jackson, M.: Glaciological investigations in Norway 2018. NVE Rapport no. 46/2019, http://publikasjoner.nve.no/rapport/2019/rapport2019_46.pdf, 2019.

Kjøllmoen, B. (Ed.), Andreassen, L.M., Elvehøy, H.: Glaciological investigations in Norway 2024. NVE Rapport 27/2025, Norwegian Water Resources and Energy Directorate, https://doi.org/10.58059/2xvm-1x48, 2025.

Kristensen, E. and Andreassen L.M.: Vanishing Ice Patches and Archaeological Potential? Annals of Glaciology, e6, https://doi.org/10.1017/aog.2026.10039, 2026

Kuhn, M.: The mass balance of very small glaciers. – In: Zeitschrift für Gletscherkunde und Glazialgeologie 31, 1-2: 171-179, 1995.

Lapazaran, J. J., Otero, J., Martín-Español, A., and Navarro, F. J.: On the errors involved in ice-thickness estimates I: ground-penetrating radar measurement errors. Journal of Glaciology, 62(236), 1008–1020. https://doi.org/10.1017/jog.2016.93, 2016.

Lilien, D. A., Hills, B. H., Driscol, J., Jacobel, R., and Christianson, K.: ImpDAR: an open-source impulse radar processor. Annals of Glaciology, 61(81), 114–123, doi: 10.1017/aog.2020.44, 2020.

https://doi.org/10.5194/egusphere-2026-3152
Preprint. Discussion started: 29 June 2026

Lilleøren, K.S., Etzelmüller, B., Schuler, T.V., Gisnås, K., and Humlum, O.: The relative age of mountain permafrost—estimation of Holocene permafrost limits in Norway. Global and Planetary Change, 92, 209-223, 2012.

Lussana, C., Tveito, O. E., Dobler, A., and Tunheim, K.: SeNorge_2018, daily precipitation, and temperature datasets over Norway. Earth System Science Data, 11, 1531–1551, ISSN 18663516, doi:10.5194/essd-11-1531-2019, 2019.

Mott, R., Vionnet, V., and Grünewald, T.: The Seasonal Snow Cover Dynamics: Review on Wind-Driven Coupling Processes. Frontiers in Earth Science, 6, ISSN 22966463, doi:10.3389/feart.2018.00197, 2018.

Navarro, F. and Eisen, O.: Ground-penetrating radar in glaciological applications, in: Remote sensing of glaciers: Techniques for topographic, spatial and thematic mapping of glaciers, Taylor & Francis London, 195–229, https://doi.org/10.1201/b10155, 2009.

Nesje, A., Pilø, L. H., Finstad, E., Solli, B., Wangen, V., Ødegård, R. S., Isaksen, K., Støren, E. N., Bakke, D. I., and Andreassen, L. M.: The climatic significance of artefacts related to prehistoric reindeer hunting exposed at melting ice patches in southern Norway. The Holocene, doi: 10.1177/0959683611425552, 2011.

Oerlemans, J. and Klok, E. J.: Effect of summer snowfall on glacier mass balance, Annals of Glaciology, 38(1), 97–100. https://doi.org/10.3189/172756404781815158, 2004.

Ohmura, A.: Physical basis for the temperature-based melt-index method, Journal of applied Meteorology, 40(4), 753-761, 2001.

Ord, J.K. and Getis, A.: Local Spatial Autocorrelation Statistics: Distributional Issues and an Application. Geographical Analysis, 27, 286-306, 1995.

Paasche, Ø., Hanssen-Bauer, I., Andreassen, L.M., Bakke, S.J., Dyrrdal, A.V., Isaksen, K., Lutz, J.: De lange linjene, in Dyrrdal, A.V., Bakke, S.J., Hanssen-Bauer, I., Mayer, S., Nilsen, I.B., Nilsen, J.E.Ø., Paasche, Ø., Saloranta, T., Årthun, M. (Editors). Klima i Norge – kunnskapsgrunnlag for klimatilpasning oppdatert i 2025, NCCS-rapport 1/2025, https://doi.org/10.60839/4rgq-nn84, 2025

Pilø, L. H.: The archaeology of glaciers and ice patches: The intersection of climate change, glacier retreat and cultural heritage. Annals of Glaciology, 67, e5, https://doi.org/10.1017/aog.2026.10040, 2026.

https://doi.org/10.5194/egusphere-2026-3152
Preprint. Discussion started: 29 June 2026

Pilø, L., Reitmaier, T., Fischer, A., Barrett, J. H., and Nesje, A.: Ötzi, 30 years on: A reappraisal of the depositional and post-depositional history of the find, The Holocene, https://doi.org/10.1177/09596836221126133, 2022.

Saloranta, T. M.: Operational snow mapping with simplified data assimilation using the seNorge snow model. Journal of Hydrology, 538, 314–325, ISSN 00221694, doi:10.1016/j.jhydrol.2016.03.061, 2016.

Sauter, T., Brock, B. W., Collier, E., Goger, B., Groos, A. R., Haualand, K. F., Mott, R., Nicholson, L., Prinz, R., Shaw, T. E., Stiperski, I., Georgi, A., Haugeneder, M., Mandal, A., Reynolds, D., Saigger, M., Sicart, J. E., and Voordendag, A.: Glacier-atmosphere interactions and feedbacks in high-mountain regions - A review. Reviews of Geophysics, 64, e2024RG000869. https://doi.org/10.1029/2024RG000869, 2026.

Serrano, E., González-trueba, JJ., Sanjosé, JJ., and Del Río, LM.: Ice patch origin, evolution and dynamics in a temperate high mountain environment: the Jou Negro, picos de Europa (nw Spain). Geografiska Annaler. Series A, Physical Geography, 93, 2, 57–70. JSTOR http://www.jstor.org/stable/41236793, 2011.

Sollid, J. L., Holmlund, P., Isaksen, K., and Harris, C.: Deep permafrost boreholes in western Svalbard, northern Sweden and southern Norway. Norsk Geografisk Tidsskrift - Norwegian Journal of Geography, 54(4), 186–191, doi:10.1080/002919500448567, 2000.

Tajet, H. T. T., Benestad, R., Dobler, A., Dyrrdal, A. V., Engeland, K., Gangstø, R., Gjelten, H. M., Hanssen-Bauer, I., Lutz, J., Mayer, S., Nordli, Ø., Paasche, Ø., Tveito, O. E., Ødemark, K.: Temperatur in Dyrrdal, A. V., Bakke, S. J., Hanssen-Bauer, I., Mayer, S., Nilsen, I. B., Nilsen, J. E. Ø., Paasche, Ø., Saloranta, T., Årthun, M. (redaktører). Klima i Norge – kunnskapsgrunnlag for klimatilpasning oppdatert i 2025, NCCS-rapport 1/2025, NCCS-rapport 1/2025, https://doi.org/10.60839/4rgq-nn84, 2025.

Terratec.: Rapport for luftbåren laserskanning. Juvfonne. 2019, Terratec rapport, 2019.

Terratec.: Laserskanning for nasjonal detaljert høydemodell, Terratec rapport, 2020a.

Terratec.: Laserskanning rapport. NDH Jostedalsbreen 2pkt 2020. Nord-Gudbrandsdal Laser 5pk 2020, Terratec rapport, 2020b.

https://doi.org/10.5194/egusphere-2026-3152
Preprint. Discussion started: 29 June 2026

Van Tricht, L., Zekollari, H., Huss, M., Rounce, D. R., Schuster, L., Aguayo, R., Schmitt, P., Maussion, F., Tober, B., Farinotti, D.: Peak glacier extinction in the mid-twenty-first century. Nat. Clim. Chang. https://doi.org/10.1038/s41558-025-02513-9, 2025.

Ødegård, R. S., Nesje, A. Isaksen, K., Andreassen, L. M., Eiken, T., Schwikowski, M., and C. Uglietti, C.: Climate change threatens archaeologically significant ice patches: insights into their age, internal structure, mass balance and climate sensitivity, The Cryosphere, 11, 17-32, doi:10.5194/tc-11-17-2017, 2017.

Østrem, G. and Ziegler, T.: Atlas over breer i Sør-Norge (Atlas of glaciers in South Norway), Hydrologisk avdeling, Norges Vassdrags- og Elektrisitetsvesen, Meddelelse, Oslo, Norway, 20, https://publikasjoner.nve.no/breatlas/breatlas.SoerNorge.high.res.1969.pdf, 1969.

Østrem, G., Dale Selvig, K., and Tandberg, K.: Atlas over breer i Sør-Norge (Atlas of glaciers in South Norway), Hydrologisk avdeling, Norges Vassdrags- og Energiverk, Meddelelse, Oslo, Norway, 61, https://publikasjoner.nve.no/breatlas/breatlas.SoerNorge.high.res.1988.pdf, 1988.

Winsvold, S. H., Andreassen, L.M., and Kjøllmoen, B.: Northernmost no more? The fragmentation of Nordmannsjøkelen in Norway, Annals of Glaciology, 67, e12, https://doi.org/10.1017/aog.2026.10047, 2026.

Zekollari, H, Schuster, L., Maussion, F., Hock, R., Marzeion, B., Rounce, D. R., Compagno, L., Fujita, K., Huss, M., James, M., Kraaijenbrink, P. D. A., Lipscomb, W. H., Minallah, S., Oberrauch, M., Tricht, L. V., Champollion, N., Edwards, T., Farinotti, D., Immerzeel, W., Leguy, G., and Sakai, A.: Glacier preservation doubled by limiting warming to 1.5°C versus 2.7°C, Science 388, 979–983. doi:10.1126/science.adu4675, 2025.